Fast local warming ~~of sea-surface~~ is the main ~~factor~~ driver of recent deoxygenation in the northern Arabian Sea

Zouhair Lachkar[1], Michael Mehari[1], Muchamad Al Azhar[1,4], Marina Lévy[2], and Shafer Smith[1,3]

[1]Center for Prototype Climate Modeling, New York University Abu Dhabi, Abu Dhabi, UAE
[2]Sorbonne Université (CNRS/IRD/MNHN), LOCEAN-IPSL, Paris, France
[3]Courant Institute of Mathematical Sciences, New York University, New York, USA
[4]Plymouth Marine Laboratory, Plymouth, UK

Correspondence: Zouhair Lachkar (zouhair.lachkar@nyu.edu)

Abstract.

The Arabian Sea (AS) hosts one of the most intense oxygen minimum zones (OMZs) in the world. Observations ~~show~~ suggest a decline of O_2 in the northern AS over the recent decades accompanied by an intensification of the suboxic conditions there. Over the same period, the local sea-surface temperature has risen significantly, particularly over the Arabian Gulf (also known as Persian Gulf, hereafter the Gulf), while summer monsoon winds may have intensified. Here, we ~~reconstruct~~ simulate the evolution of dissolved oxygen in the AS from 1982 through 2010 and explore its controlling factors, with a focus on changing atmospheric conditions. To this end, we use a set of eddy-resolving hindcast simulations forced with ~~observation-based~~ winds and heat and freshwater fluxes from an atmospheric reanalysis. We find a significant deoxygenation in the northern AS with O_2 inventories north of 20°N dropping by over ~~2~~6% decade^{-1} ~~and 7% decade^{-1} in the top 200~~between 100 and 1000 m~~and the 200-1000 m layer, respectively~~. These changes cause an expansion of the OMZ volume north of 20°N at a rate of 0.6% decade^{-1} as well as an increase in the volume of suboxia and the rate of denitrification by ~~10~~14% decade^{-1} and ~~13~~15% decade^{-1}, respectively. We also show that strong interannual and decadal variability modulate dissolved oxygen in the northern AS with most of the O_2 decline taking place in the 1980s and 1990s. Using a set of sensitivity simulations we demonstrate that deoxygenation in the northern AS is essentially caused by ~~a~~ reduced ventilation induced by the recent fast warming of the sea surface, ~~in particular in the Gulf. Concomitant~~ including in the Gulf, with a contribution from concomitant summer monsoon wind intensification~~contributes to deoxygenation at depth and in the upper ocean north of 20°N but enhances oxygenation of the upper ocean elsewhere~~. This is because, on the one hand, surface warming enhances vertical stratification ~~, thus limiting~~ and increases Gulf water buoyancy, thus inhibiting vertical mixing and ventilation of the ~~intermediate ocean, while~~ thermocline. On the other hand, summer monsoon wind intensification causes a rise of the thermocline depth ~~to rise~~ in the northern AS ~~and deepen elsewhere, thus contributing to lowering~~ that lowers O_2 levels in the upper ~~200 m in the northern AS and increasing it in the rest of the AS~~ocean. Our findings confirm that the AS OMZ is strongly sensitive to upper-ocean warming and concurrent changes in the Indian monsoon winds. Finally, our results also demonstrate that changes in the local climatic forcing play a key role in regional dissolved oxygen changes and hence need to be properly represented in global models to reduce uncertainties in future projections of deoxygenation.

1 Introduction

Rising ocean temperatures decrease O_2 solubility in seawater, increase respiration-driven oxygen consumption and enhance vertical stratification, thus reducing interior ocean ventilation (Oschlies et al., 2018). These changes collectively cause the ocean to lose oxygen as it warms up, a process termed ocean deoxygenation. Observational and modeling evidence suggest that the majority of the observed oxygen decline is caused by changes in ocean ventilation and biogeochemistry (Bindoff et al., 2019). Over the last five to six decades, the global ocean oxygen content has dropped by 2% (Ito et al., 2017; Schmidtko et al., 2017), a tendency predicted to accelerate in the future in response to ocean warming. ~~Although global models generally misrepresent the observed regional patterns of deoxygenation and underestimate its rate (Oschlies et al., 2018), they all consistently predict further deoxygenation in the future irrespective of the chosen CO_2 emission scenario (Bopp et al., 2013; Cocco et al., 2013). For instance, the Earth system models from the Coupled Model Intercomparison Project Phase 5 (CMIP5) predict a decline of dissolved~~ In the upper 1000 m, a growing consensus points towards a loss of O_2 of ~~-3.45 ±0.44% by the end of the twenty-first century under the RCP8.5 emission scenario (Bopp et al., 2013). Models from the more recent Coupled Model Intercomparison Project Phase 6 (CMIP6) with generally higher horizontal resolution, more complex biogeochemical models and improved representation of O_2 in the subsurface (Séférian et al., 2020) show a rate of deoxygenation in the 100-600 m subsurface layer that is up to 40% faster than in the CMIP5-based projections (Kwiatkowski et al., 2020)~~0.5-3.3% between 1970-2010 (Bindoff et al., 2019). However, the analysis of local time series suggests much stronger trends at particular sites (Whitney et al., 2007; Bograd et al., 2015). Ocean deoxygenation can cause the expansion of naturally-occurring low-O_2 water bodies known as Oxygen Minimum Zones (OMZs) ~~(Stramma et al., 2008; Breitburg et al., 2018), and has already led to the quadrupling of the volume of anoxic waters since 1960 (Schmidtko et al., 2017)~~(Stramma et al., 2008; Breitburg et al., 2018; Bindoff et al., . This can increase the frequency and intensity of hypoxic events, stressing sensitive organisms and causing loss of marine biodiversity and shifts in the food web structure (Rabalais et al., 2002; Vaquer-Sunyer and Duarte, 2008; Laffoley and Baxter, 2019). ~~Finally, it has been reported that ocean deoxygenation may cause some oceanic regions to transition to anoxia in the future (Bristow et al., 2017).~~

The Arabian Sea (AS) hosts one of the world's largest and most extreme OMZs, with suboxia ($O_2 < 4$ mmol m^{-3}) prevailing across most of the intermediate ocean (from 150 down to 1,250 m) in its northern and northeastern parts, turning it in a global hotspot of denitrification (Bange et al., 2005; Codispoti et al., 2001). ~~The~~ Because of the challenges associated with data sparsity, the previously documented O_2 changes in the AS depict a complex picture with no consistent trends across the entire region ~~(Laffoley and Baxter, 2019)~~(Laffoley and Baxter, 2019; Bindoff et al., 2019). Yet, there is mounting evidence for a decline of O_2 concentrations in the northern ~~and western~~ AS over the last few decades. For example, the global analysis of historical oxygen observations by Ito et al. (2017) reveals a moderate drop of O_2 levels in the subsurface of the AS between 1960 and 2010. The analysis of available O_2 observations by Schmidtko et al. (2017) similarly indicates a decline of oxygen in the northern and western AS as well as along the west coast of India between 1960 and 2010. In an analysis of over 2000 O_2 profiles collected during 53 oceanographic expeditions that took place between 1960 and 2008 off the coast of Oman, Piontkovski and Al-Oufi (2015) documented a decline of O_2 in the upper 300 m in the northern and northwestern AS

that they attributed to increased thermal stratification and a shoaling of the oxycline between 1960s and years 2000s. Banse et al. (2014) analyzed discrete historical O_2 measurements collected in the central and southern AS in the 150-500 m layer between 1959 and 2004. They found no clear systematic trend across the entire AS, although O_2 was found to decline in most of the central AS and slightly increase in the southern AS (between 8-12°N). Because of the sparsity of observations, these trends were generally based on a small number of samples and not always statistically significant. Authors in this study also analyzed trends in subsurface nitrite (NO_2^-) concentrations, typically used as a proxy of the presence of suboxia and denitrification at depth. They found both positive and negative trends in different locations with a larger number of profiles indicating an increase in nitrite concentrations over time, suggesting an overall intensification of the OMZ over the study period. do Rosário Gomes et al. (2014) reported a radical shift in the winter bloom dominant phytoplankton species from diatoms to large dinoflagellate, Noctiluca scintillans, which they linked to a decline of O_2 concentrations in the region~~over the same period~~. More recently, using sea glider data and historical observations, Queste et al. (2018) showed an intensification of the suboxic conditions at depth in the Gulf of Oman over the last three decades. Although there has been little work done on documenting potential deoxygenation in the Arabian marginal seas (i.e., the Red Sea and the Gulf), preliminary observations suggest ongoing deoxygenation in the Gulf with recent emergence of summertime hypoxia documented there (Al-Ansari et al., 2015; Al-Yamani and Naqvi, 2019).

In addition to changes in O_2, the AS has undergone ~~several~~ major environmental changes over the recent decades that may intensify in the future. In particular, the AS has experienced a strong warming throughout most of the twentieth century that has accelerated since the early 1990s ~~(Kumar et al., 2009)~~(Kumar et al., 2009; Gopika et al., 2020). The warming has been particularly fast in the two Arabian marginal seas (i.e., the Red Sea and the Gulf) over the last three decades with warming rates reaching up to 0.17 ± 0.07°C decade^{-1} and 0.6 ± 0.3°C decade^{-1} in the two semi-enclosed seas, respectively (Chaidez et al., 2017; Strong et al., 2011; Al-Rashidi et al., 2009). ~~This is twice to three times faster than the global average.~~ The AS warming has been ~~associated with important ecological~~ linked to important physical and biogeochemical changes. For instance, using satellite observations and a set of historical simulations of the northern Indian Ocean, Roxy et al. (2016) found a drop of summer productivity by up to 20% between 1950 and 2005 in the western AS that they linked to surface warming and increased stratification. ~~Furthermore, the strong~~ Goes et al. (2020) reported an increase in winter stratification associated with a weakening of winter convective mixing in the northern AS. These authors also presented observational evidence of a strong loss of inorganic nitrogen in the AS over the recent decades that they linked to enhanced denitrification driven by OMZ intensification. These changes have been suggested to favor winter blooms of the mixotroph Noctiluca scintillans at the expense of diatoms (Goes et al., 2020). The Gulf warming has ~~been linked to~~ also been associated with important ecological and biogeochemical changes such as recent frequent mass coral bleaching events ~~there (Burt et al., 2019) . Additionally, using a set of idealized model simulations, Lachkar et al. (2019) found the warming of the Gulf to induce a~~ (Burt et al., 2019) as well as a potential reduction of the ventilation of the AS OMZ ~~, thus causing its intensification. Important~~ (Lachkar et al., 2019). Finally, important changes in the ~~regional~~ summer monsoon winds have also been reported. For instance, ~~Goes et al. (2005) have documented an increase in~~ Sandeep and Ajayamohan (2015) described a poleward shift in the monsoon low level jet stream over the recent decades that is expected to intensify in the future. This would lead to an intensification (resp. weakening) of summer monsoon

winds off the coast of Oman (resp. Somalia). Praveen et al. (2016) suggested the Oman coast is to experience a future increase in summer upwelling accompanied with an enhancement of summer productivity whereas deCastro et al. (2016) predicted a future strengthening of the Somali coastal upwelling based on an ensemble of global and regional model simulations for the 21st century. Yet, other studies reported a decline in the intensity of summer monsoon ~~wind intensity off Somalia between 1997 and 2005. Other studies have also suggested a climate change driven intensification of the summer monsoon~~ winds~~(Wang et al., 2013) and weakening of winter monsoon winds (Vallivattathillam et al., 2017) in the northern AS. Finally, Lachkar et al. (2018) found a tight link between the strength of the monsoon winds and the depth and intensity of the AS OMZ~~. For instance, Swapna et al. (2017) suggested a weakening of the summer monsoon circulation over the recent decades. The analysis of a selected set of CMIP5 models by Sooraj et al. (2015) also suggests a future weakening of the Asian Summer monsoon circulation south of 10°N. However, this study also projects an intensification of the summer monsoon circulation north of 10°N associated with a northward shift of the monsoon circulation in agreement with previous CMIP5 model analyses.

While these environmental perturbations may have contributed to the observed O_2 decline ~~over the recent decades~~in the northern AS, their potential interactions and the mechanisms through which they act to modulate O_2 remain ~~largely~~ poorly understood. In particular, the respective roles of recent surface warming on the one hand and summer monsoon wind intensification on the other hand are yet to be quantified. Moreover, the potential contribution of the recent fast warming of the Gulf to the declining O_2 levels in the northern AS has not yet been investigated. Here we reconstruct the trends in O_2 over the period between 1982 and 2010 using a high-resolution hindcast simulation of the Indian Ocean and examine their physical and biogeochemical drivers using a set of sensitivity experiments. We show that recent deoxygenation in the northern AS has been caused essentially by surface warming, ~~in particular in the Gulf~~ with a significant contribution from the Gulf warming, bringing about a reduction in the ventilation of the subsurface and intermediate layers. We also show that summer monsoon intensification enhanced oxygenation of the upper ocean south of 20°N but has contributed to deoxygenation in the northern AS. These changes are likely to have important ecological and biogeochemical consequences.

2 Methods

2.1 Models

The circulation model is the Regional Ocean Modeling System (ROMS)-AGRIF version (http://www.croco-ocean.org) configured for the Indian Ocean. It uses the free-surface, hydrostatic, primitive equations in a rotating environment and has a terrain-following vertical coordinate system (Shchepetkin and McWilliams, 2005). To limit diapycnal mixing errors, the diffusive component of the rotated, split, upstream-biased, 3rd order (RSUP3) tracer advection scheme is rotated along geopotential surfaces (Marchesiello et al., 2009). The non-local K-Profile Parameterization (KPP) scheme is used to parametrize subgrid vertical mixing (Large et al., 1994). The model domain covers the full Indian Ocean from 31°S to 31°N and 30°E to 120°E with a 1/10° horizontal resolution and 32 sigma-coordinate vertical layers with enhanced resolution near the surface. The biogeochemical model is a nitrogen-based nutrient-phytoplankton-zooplankton-detritus (NPZD) model (Gruber et al., 2006). It is based on a system of ordinary differential equations representing the time-evolution of seven state variables: two nutrients

(nitrate and ammonium), one phytoplankton class, one zooplankton class, two classes of detritus (small and large sizes) and a dynamic chlorophyll-to-carbon ratio. The model has a module describing the cycling of oxygen as well as a parameterization of water-column and benthic denitrification (Lachkar et al., 2016).

2.2 Experimental design

The hindcast simulation is forced with ECMWF ERA-Interim 6-hourly heat fluxes, air temperature, pressure, humidity, precipitation and winds over the period from January 1982 to December 2010. Sea surface temperature (SST) is restored to AVHRR-Pathfinder and Aqua-Modis observations and surface salinity is restored to the Simple Ocean Data Assimilation (SODA) reanalysis data using kinematic heat and freshwater flux corrections proposed by Barnier et al. (1995). Initial and lateral boundary conditions for temperature, salinity, currents and sea surface height are computed from the SODA reanalysis (Carton and Giese, 2008). The initial and lateral boundary conditions for nitrate and oxygen are extracted from the World Ocean Atlas (WOA) 2013 (Garcia et al., 2013a, b). Finally, we used a monthly climatological runoff and annual river nutrient discharge from major rivers in the northern Indian Ocean (including the Indus and Narmada rivers flowing into the Arabian Sea) derived from available observations and a global hydrological model (Ramesh et al., 1995; Dai and Trenberth, 2002; Krishna et al., 2016). We restrict our analysis to the AS region extending from ~~5~~3.5°S to 30°N in latitude and from 32°E to ~~78~~76°~~W~~ E in longitude (Fig S1, Supporting Information (SI)).

~~**Evaluation of model simulated oxygen** Annual mean O_2 averaged between 250 m and 700 m (in mmol m^{-3}) as simulated in the model (right) and from the WOA-2018 dataset (left).~~

The model is spun-up using climatological forcing during 58 years and is then run for four 29-year (1982-2010) repeating forcing cycles, with the first three cycles used as a part of the spin-up period (i.e., the total duration of the spin-up phase is 145 years) and the forth cycle used for analysis (similar to the forcing protocol used in the Ocean Model Intercomparison Project, Griffies et al., 2016). The climatological run is extended for an additional 29 years to quantify the artificial trends purely driven by the model drift and contrast them to trends estimated in our hindcast run. The analysis of model drift indicates a very negligible drift in salinity by the end of the climatological forcing period (Fig S2, SI). For O_2, the model drift decreases but remains positive (ocean oxygenation) by the end of the climatological forcing spin-up period, suggesting that the estimated deoxygenation rates extracted from our ~~hidncast~~ hindcast simulation are rather conservative (Figs S2-S5, SI). A detailed description of the model drift is presented in the SI.

2.3 Model evaluation

We use available in-situ and satellite-based observations to evaluate the performance of the model in capturing the spatial ~~and~~ patterns as well as the seasonal variability in key physical and biogeochemical properties. We ~~first~~ evaluate the mean state by contrasting a model climatology computed over the (1982-2010) study period to available observation-based climatologies.

~~The model reproduces well the observed distributions of sea surface temperature (SST) inferred from the Advanced Very High Resolution Radiometer (AVHRR) satellite data in both winter and summer seasons (Fig 1). In particular~~The details of this evaluation are presented in the SI. Despite a few identified biases, the model ~~captures the intense temperature gradients~~

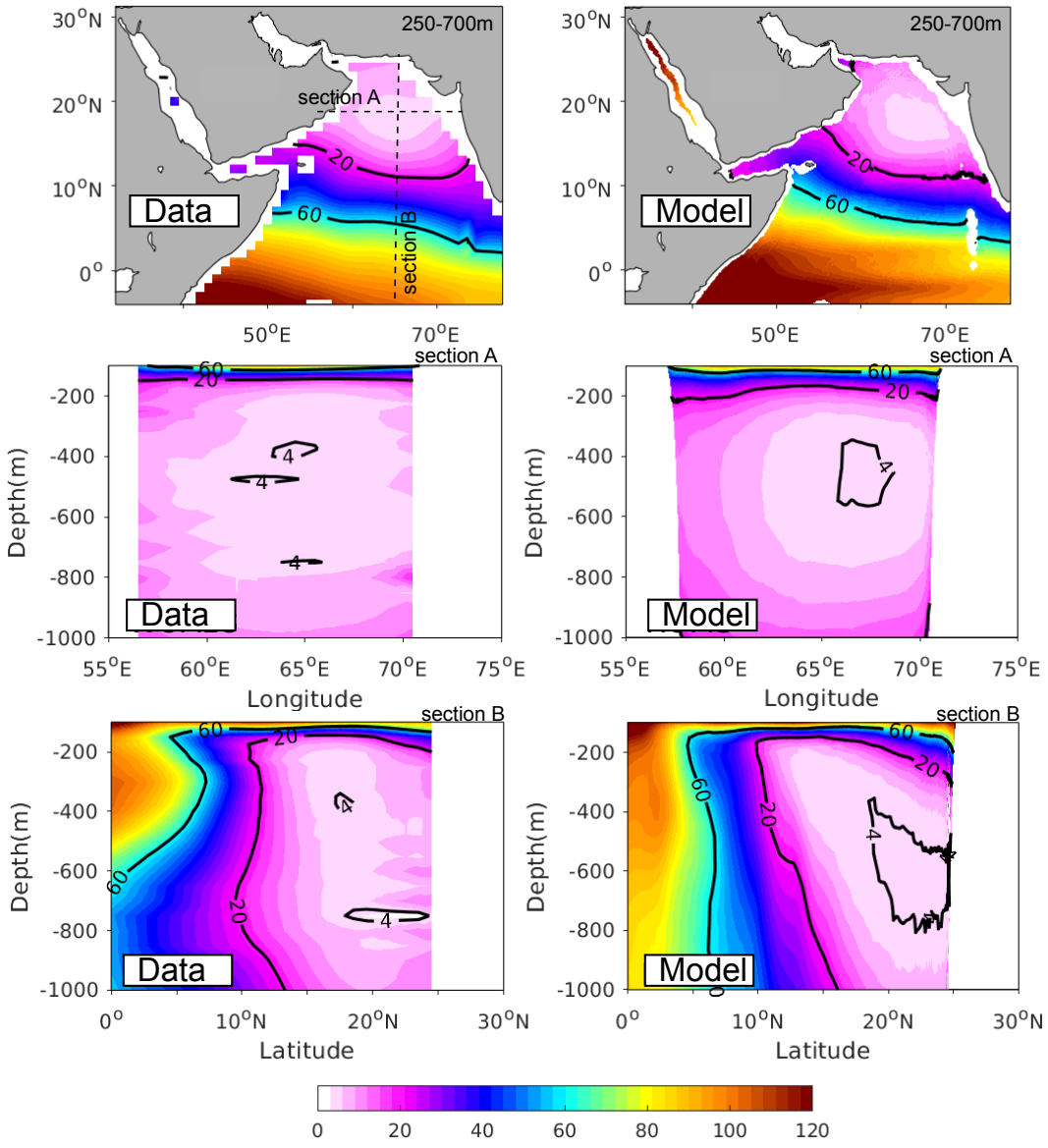

Figure 1. ~~Evaluation of model simulated sea surface temperature and salinity~~ **Evaluation of simulated oxygen** Annual mean O_2 (~~a-d) Sea surface temperature (~~in ~~°C~~mmol m^{-3}) ~~as simulated in the model (right~~top) averaged between 250 m and ~~from the AVHRR satellite product~~ 700 m and along (~~left~~middle) ~~in winter (top)~~ zonal section A at 18°N and ~~summer~~ (bottom) ~~monsoon seasons.(e-h) Sea surface salinity (in PSU)~~ meridional section B at 65°E as simulated in the model (right) and from the WOA-2018 dataset (left)~~in winter (top) and summer (bottom) monsoon seasons~~.

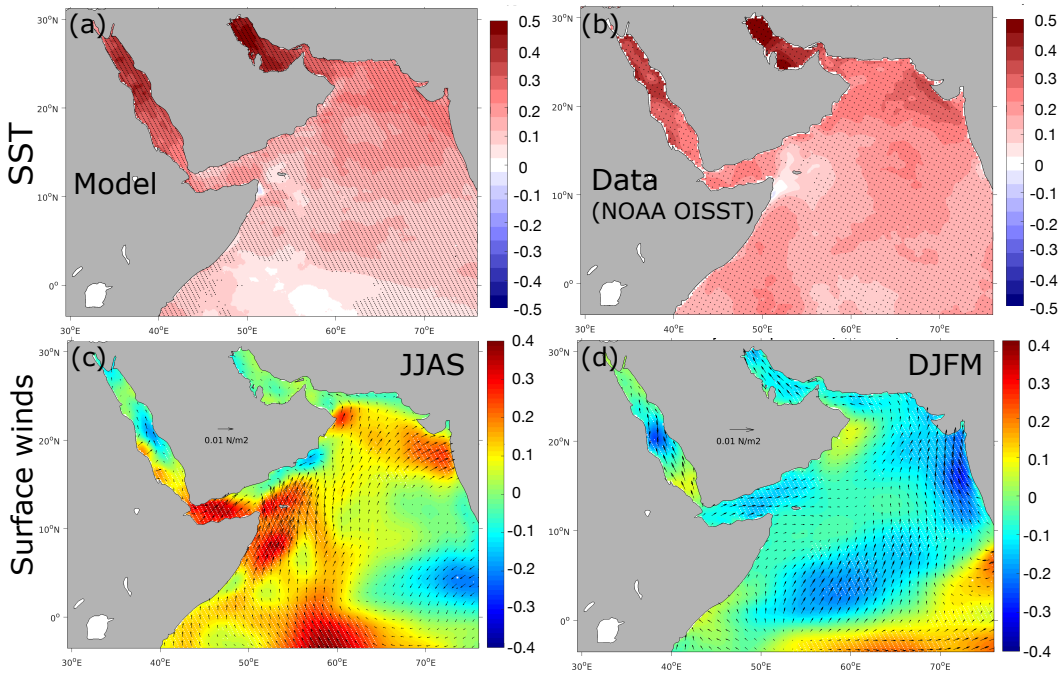

Figure 2. ~~**Evaluation of model simulated surface currents** Surface currents~~ **Warming and surface wind trends.** (a-b) Linear trends in ~~m s~~sea surface temperature (in °C decade^{-1}) as simulated ~~in~~ by the model (~~right~~a) and from the NOAA OISST data product. (c-d) trends in ERA-Interim surface ~~drifter climatology of Lumpkin and Johnson (2013)~~ winds in summer (~~left~~c) ~~during~~ and winter (~~top~~d)~~and summer~~. Color shading indicates trends in wind speed (~~bottom~~in m s^{-1} decade^{-1}) ~~monsoon seasons~~whereas arrows show trends in wind stress vector. Statistically significant trends at 95% confidence interval following a Mann-Kendall (MK) test are represented by stippling.

~~prevailing in both seasons across the AS.Indeed, the model reproduces the strong temperaturecontrasts between the AS and its marginal seas,~~ exhibits reasonable skill in reproducing the mean seasonal climatological state for both physical (i.e., temperature, salinity, currents) and biogeochemical properties (i.e., nitrate, chlorophyll; see Figs S6-S10, SI). Furthermore, the model reproduces fairly well the ~~Gulf and the Red Sea as well as the upwelling-driven cold SST tongue that develops in the west AS during summer. Similarly, the distribution of the mean surface salinity is in a good agreement with that from the WOA2018 climatology~~ size, intensity and vertical structure of the AS oxygen minimum zone (Fig 1). ~~The AS surface circulation is similarly well represented in the model in both summer and winter seasons (Fig 2). In particular, the model simulates well the reversal of the Somali Current between summer and winter seasons~~

We also evaluate the model performance in reproducing observed long term changes. To this end, we evaluate the model simulated long-term evolution of temperature and salinity at multiple depths as well as the ~~prominent features of the surface circulation system including the Southern Gyre, the Great Whirl and the Southwest Monsoon Current in summer and the Northeast Monsoon Current and South Equatorial Countercurrent in winter (Schott et al., 2009).~~

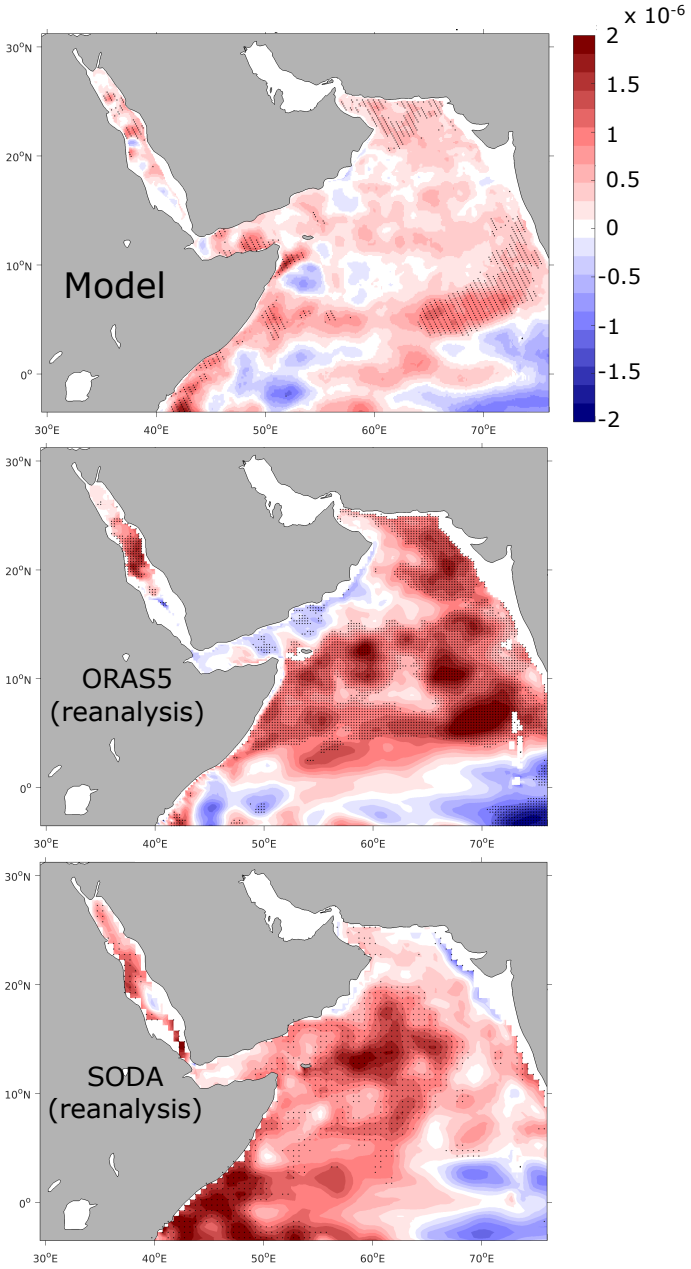

Figure 3. ~~**Evaluation of model simulated surface nitrate and chlorophyll-a** (a-d) Surface NO_3^- (~~**Trends in upper ocean vertical stratification** Linear trends in ~~mmol m^{-3}) as simulated in the model~~ static stability $E = \frac{-1}{\sigma}\frac{\partial \sigma}{\partial z}$ (~~right)~~ with σ the density of the water and ~~from~~ z the ~~WOA-2018 dataset (left~~depth) ~~in winter~~ at 100 m (~~top) and summer (bottom) monsoon seasons. (e-h) Sea surface chlorophyll-a concentrations (~~in ~~mg~~ m^{-3}~~$^{-1}$ decade^{-1}) between 1982 and 2010 as simulated in ~~the model~~ ROMS (~~right~~top) and from ~~SeaWiFS climatology~~ ORAS5 (~~left~~middle) ~~during winter (top)~~ and ~~summer~~ SODA (bottom) ~~monsoon seasons~~reanalyses. Statistically significant trends at 95% confidence interval following a Mann-Kendall (MK) test are represented by stippling.

The model reproduces relatively well the observed surface distribution of nitrate in both seasons, despite a tendency towards slightly overestimating surface concentrations in the oligotrophic open ocean and underestimating them in the northern AS during summer (Fig 3). The large-scale nitrate distribution at depth is also well captured by the model despite some local biases (Fig S6changes in the upper ocean vertical stratification and surface chlorophyll-a concentration. More specifically, we contrast simulated trends in SST to trends based on four observational SST products: AVHRR (used to force the model), ERA5 (Merchant et al., 2014), HadISST (Rayner et al., 2003) and the NOAA OISST blended product (Huang et al., 2021). This comparison reveals that the model simulated warming agrees relatively well with that from the different SST products, despite differences in the magnitude of warming, with ERA5 (resp. HadISST) displaying the strongest (resp. weakest) rates of warming (Fig 2 and Fig S11, SI). The model reproduces the observed high chlorophyll-a concentrations associated with the winter and summer blooms Furthermore, we also contrast the interannual anomalies in temperature and salinity in the northern and western AS , respectively (Fig 3). Furthermore, summer high chlorophyll concentrations off the Indian west coast are also relatively well captured by the model. In contrast, the model tends to substantially overestimate chlorophyll levels off the Somali coast and in the western AS in general. This discrepancy may result from the fact that the model does not represent iron and silicic acid that may be contributing to limiting productivity in this region (Koné et al., 2009). Finally, the model captures fairly well the large-scale distribution of oxygen in the AS region (Fig 4). In particular, the location, size and intensity of the AS oxygen minimum zone is relatively well reproduced.

A more quantitative assessment of the model performance is shown using Taylor diagrams (Taylor, 2001) that summarize three important statistics: (i) the correlation coefficient between the model and the observations, (ii) the standard deviation in the model relative to the observations and (iii)the centered root mean square (RMS) with respect to observations (Fig 5). To this end, in-situ observations from the World Ocean Database (2018) were binned temporally and spatially into a 0.5AS in the model to those from WOD2018 observations at different depths (Fig S12 and Fig S13, SI). This comparison reveals that in the northern AS the simulated and observed trends in upper ocean temperature agree well. Indeed, the linear trends in temperature amount to +0.11° x 0.5C per decade at the surface (resp. +0.12° seasonal climatology covering the AS region. No spatial interpolation was performed and the modeland observations are contrasted at the observation points only. This analysis confirms the relatively good agreement between model and observations. More specifically, it shows that surface temperature and salinity, as well as upper (400 m) ocean nitrate and O_2 distributions generally all agree well with observations with correlations above 0.9 and comparable standard deviations, across all seasons (Fig 5). The model shows a weaker performance though in simulating surface chlorophyll with correlations ranging from 0.42 during winter months to 0.67 during the Fall season (Fig 5).

Finally, we evaluate the model performance in reproducing observed long term changes. To this end, we binned observations from the World Ocean Database (2018) seasonally on a 5C per decade at 100m) in the model and +0.11° x 5C per decade at the surface (resp. +0.14° horizontal grid at each standard depth. We then computed seasonal climatologies for the first five years (1982-1986) and the last five years (2006-2010)for each bin where at least three observations were available from each year in the two periods. Using these requirements allows us to reduce the local noise in the estimated long-term changes. Yet, only temperature was found to have a coverage that is sufficiently dense to enable these anomalies to be estimated over a significant portion of the AS. Contrasting the long term temperature changes in the top C per decade at 100m) in the WOD2018

dataset (all trends are statistically significant at both depths ($p<0.01$)). In contrast, temperature trends at 200 ~~m in the model and in the observations reveals an overall good agreement in terms of~~ m are very weak and statistically non-significant in both the model and WOD2018. For salinity, both the model and the ~~magnitude and the patterns of upper ocean warming in both summer and winter seasons (Fig S7~~ WOD2018 observations suggest a slight increase in the upper ocean salinity over the study period (Fig S13, SI). Yet, the highly sparse observational coverage (most of the observations coming from the last decade of the simulation) precludes extracting meaningful trends from the data to validate the simulated salinity long-term changes (Fig S14, SI). Finally, we also evaluate the evolution of vertical stratification and static stability in the AS in the model. As salinity observations are very sparse over the region during the study period we contrast simulated vertical stratification to that from reanalysis products such as SODA and ORAS5 (Fig 3 and Fig ~~S8~~S15, SI). This comparison reveals that overall the simulated increase in vertical stratification in the AS is comparable to similar trends derived from the ORAS5 and SODA reanalyses, although with local differences in their magnitude and regional patterns. For instance, our model underestimates the magnitude of stratification increase for most of the AS domain relative to ORAS5 and in the central and western AS in comparison to SODA. For biological variables, we only evaluate interannual variability in surface chlorophyll as O_2 (and NO_3^-) observations are extremely limited in the area during the study period (Fig S14, SI). As satellite chlorophyll data is available only from september 1997, we contrast simulated chlorophyll to observations over the common period from september 1997 to the end of the year 2010. The 13-year period is too short to extract meaningful long-term trends. Yet, this comparison is still useful as it reveals a decent agreement between the model and observations over the study period with a moderate correlation of 0.48 between the modeled and observed interannual anomalies in the northern AS (Fig S16, SI).

In summary, ~~despite a few identified biases, the model exhibits reasonable skill in reproducing the mean seasonal climatological state for both physical and biogeochemical properties. Furthermore, it reproduces fairly well the structure and intensity of the AS oxygen minimum zone~~the model reproduces the observed warming trends in the upper ocean of the northern AS and captures relatively well the observed large-scale changes in vertical stratification in the region. Finally, ~~both the magnitude and patterns of the simulated upper ocean warming are consistent with observations~~the model also shows a decent skill at capturing the observed interannual variability in surface chlorophyll.

~~**Model skill assessment with Taylor diagrams.** Taylor diagram presenting statistical comparison of modeled and observed variables. Taylor (2001) diagram of sea surface temperature (blue), salinity (red), chlorophyll-a (green) and nitrate (purple) and oxygen (cyan) in the upper 400 m in (a) winter, (b) spring, (c) summer and (d) fall. The reference point in the Taylor diagram corresponds to observations. The radius (distance to the origin point) represents the modeled standard deviation relative to the standard deviation of the observations. The angle between the model point and the X-axis indicates the correlation coefficient between the model and the observations. Finally, the distance from the reference point to a given modeled field represents that field's centered root mean square (RMS) with respect to observations.~~

2.4 Trends and oxygen diagnostics

3 Results

2.1 Deoxygenation trends in the Arabian Sea

Deoxygenation rates in the AS between 1982 and 2010. (a-b) Trends in O_2 inventories (in % per decade) in (a) the top 200 m and (b) the 200-1000 m layer. (c) trends in O_2 in the upper 1000 m across 65°E (in mmol m^{-3} $decade^{-1}$). Statistically significant trends at 95% confidence interval following a Mann-Kendall (MK) test are represented by hatching (a-b) and stippling (c). The purple and cyan lines indicate the average positions of the hypoxic ($O_2 < 60$ mmol m^{-3}) and suboxic ($O_2 < 4$ mmol m^{-3}) boundaries, respectively, (a) at 100 m, (b) 500 m and (c) along 65°E.

To investigate long-term changes in O_2 time series , and other environmental properties (e.g., SST, winds, stratification, etc), data was deseasonalized by removing monthly climatologies from the original time series. Furthermore, to identify significant trends in O_2 and other environmental factors we used the non-parametric Mann-Kendall (MK) test (Mann, 1945; Kendall, 1948) that does not assume normality of data distribution and hence is less sensitive to outliers and skewed distributions. Linear trends were computed from the slope of the least squares regression line. To separate oxygen trends driven by changes in solubility (thermal effect) from those caused by changes in ocean ventilation and respiration of organic matter, we decompose the oxygen anomaly ΔO_2 as:

$$\Delta O_2 = \Delta O_2^{sat} - \Delta AOU$$

where O_2^{sat} is the oxygen saturation concentration (in mmol m^{-3}) computed at 1 atm pressure from temperature and salinity following Garcia and Gordon (1992). It corresponds to the maximum O_2 concentration in seawater at equilibrium, for a given temperature and salinity; AOU (apparent oxygen utilization) is the difference between oxygen saturation O_2^{sat} and the actual O_2 concentration ($AOU=O_2^{sat}-O_2$). It is a measure of O_2 utilization through biological activity since the water parcel was last at equilibrium in contact with the atmosphere. Therefore it is sensitive to both biological productivity and circulation (ventilation).

2.1 Quantification of the effects of changes in atmospheric forcing

The analysis of long-term trends in atmospheric forcing reveals a widespread warming of the sea surface by between 0.5 and 1°C in the northern AS and by up to 1.5°C in the Gulf and in the northern part of the Red Sea, between 1982 and 2010 (Fig 2). In addition to surface warming, surface winds have undergone important changes with an intensification of upwelling favorable winds off Somalia and Oman, in particular during the summer monsoon season (Fig 2 and Fig S17, SI). To quantify the contributions of surface warming and wind changes to deoxygenation in the AS, we performed three additional sensitivity experiments. In the first simulation, S_{bclim}, all atmospheric and lateral boundary conditions were set to vary interannually like in the control run except the heat fluxes that were extracted from a normal year (neutral with respect to major climate variability modes), 1986, and repeated every year (i.e., climatological heat fluxes). This approach allows us to filter out interannual

variability while maintaining the high-frequency variability in the forcing (e.g., Large and Yeager, 2004; Stewart et al., 2020). In the second sensitivity run, S_{hclim_AG}, the heat fluxes were similarly extracted from the year 1986 and repeated annually, but only over the Gulf region (i.e., climatological heat fluxes over the Gulf only). In a third simulation S_{wclim_JJAS} all atmospheric and lateral boundary conditions were set to vary interannually like in the control run except summer monsoon winds that were extracted from the year 1986 and repeated every year (i.e., climatological summer winds). Finally, in a forth sensitivity simulation S_{wclim_DJFM} all atmospheric and lateral boundary conditions were set to vary interannually like in the control run except winter monsoon winds that were extracted from the year 1986 and repeated every year (i.e., climatological winter winds).

3 Results

3.1 Deoxygenation trends in the Arabian Sea

The analysis of oxygen trends between 1982 and 2010 shows a decline of O_2 concentrations in ~~the northern and western AS in the upper 200~~a large portion of the AS between 100 and 1000 m (Fig. ~~6a). Below 200 m, the drop in~~ 4). O_2 ~~is particularly important in relative terms in~~ drops locally by more than 10% per decade in the northern AS ~~but other areas in the southern and southeastern AS also show negative trends although with a weaker magnitude~~ where the suboxic core of the OMZ is located (Fig. ~~6b~~4). A vertical transect at 65°E indicates that ~~in absolute terms~~ most of the O_2 decline is concentrated north of 20°N ~~in the top~~ between 100 and 300 m (Fig. ~~6c~~4). This deoxygenation results in a significant intensification of the OMZ over the three decade study period, with the volume of suboxic (O_2 < ~~4mmol~~4 mmol m^{-3}) water increasing by nearly 14% per decade north of 20°N and by around 10% per decade when considering the entire Arabian Sea domain (Fig. ~~7a~~5 and Fig S18). This causes an amplification of denitrification in the region with an increase in denitrification rates by around ~~14~~15% per decade over the same period (Fig. ~~7c).~~ 5). The evolution of the suboxic volume and denitrification also reveals strong interannual and decadal fluctuations with a strong rate of intensification of the OMZ during the 1980s and 1990s and a relative stabilization in the last decade of the simulation. Indeed, the changes in the suboxic volume and denitrification are largest between the early 1980s and early 2000s (Fig. 5). Despite deoxygenation trends dominating in the northern and ~~western~~ southern AS, local oxygenation patches are simulated in the ~~eastern, central and southern~~ central AS (Fig~~6~~. 4). This results in the net hypoxic volume (O_2 < 60 mmol m^{-3}) that defines the OMZ volume to change little over the study period (Fig ~~7b).~~ S18). When considering the northern Arabian Sea only, the hypoxic volume shows a statistically significant increase, yet at a modest rate of 1.7% over the three decades of the simulation (Fig. 5). To put these numbers in a broader context, observations suggest that the volume of the world ocean OMZs has expanded in a range of 3-8% between 1970 and 2010 (Bindoff et al., 2019). The stronger trends simulated for the suboxic volume relative to the hypoxic volume is also consistent with previous studies. For instance, it has been suggested that the volume of anoxic waters in the global ocean has quadrupled since 1960 (Schmidtko et al., 2017). Moreover, using numerical simulations, Deutsch et al. (2011) have shown that the amplitude of variations in the volume of low oxygen conditions in the global ocean increases between 1959 and 2005 from 10% for strong hypoxia (O_2 < 40 mmol m^{-3}) to

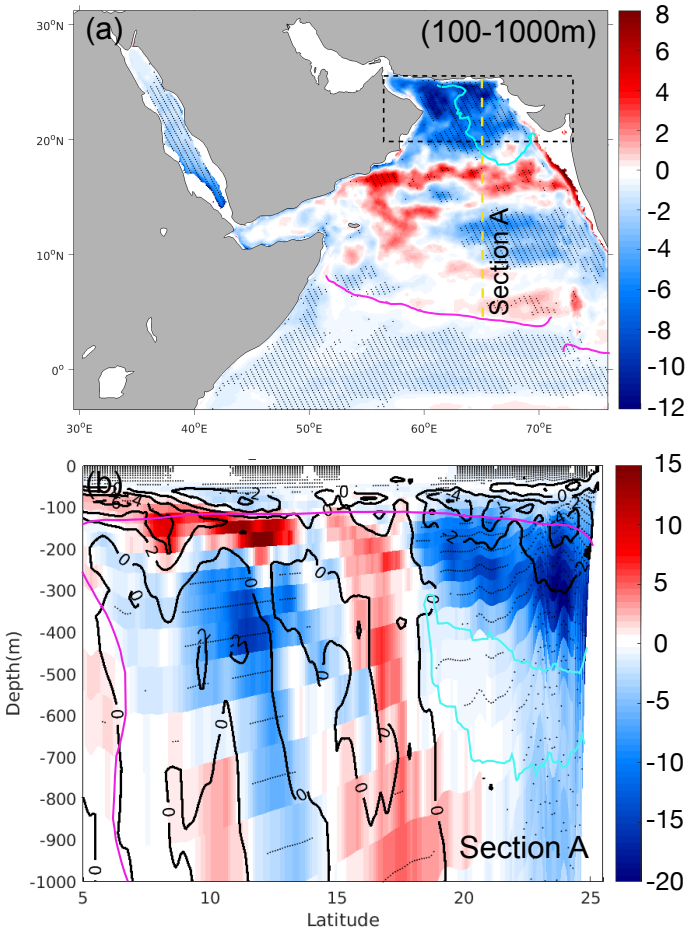

Figure 4. Deoxygenation rates in the AS between 1982 and 2010. (a) Trends in O_2 inventories (in % per decade) in the 100-1000 m layer. The black dashed line rectangle indicates the location of the northern AS box. The yellow dashed line indicates section A. (b) trends (color shading) and changes between the first five years [1982-1986] and the last five years [2006-2010] (contour lines) in O_2 in the upper 1000 m along section A at 65°E (in % per decade). Statistically significant trends at 95% confidence interval following a Mann-Kendall (MK) test are represented by hatching (a) and stippling (b). The purple and cyan lines indicate the average positions of the hypoxic ($O_2 < 60$ mmol m^{-3}) and suboxic ($O_2 < 4$ mmol m^{-3}) boundaries, respectively, at (a) 500 m and (b) along section A. Relative trends (in % per decade) were obtained by dividing the absolute trends by the local mean O_2 inventory (a) or concentration (b).

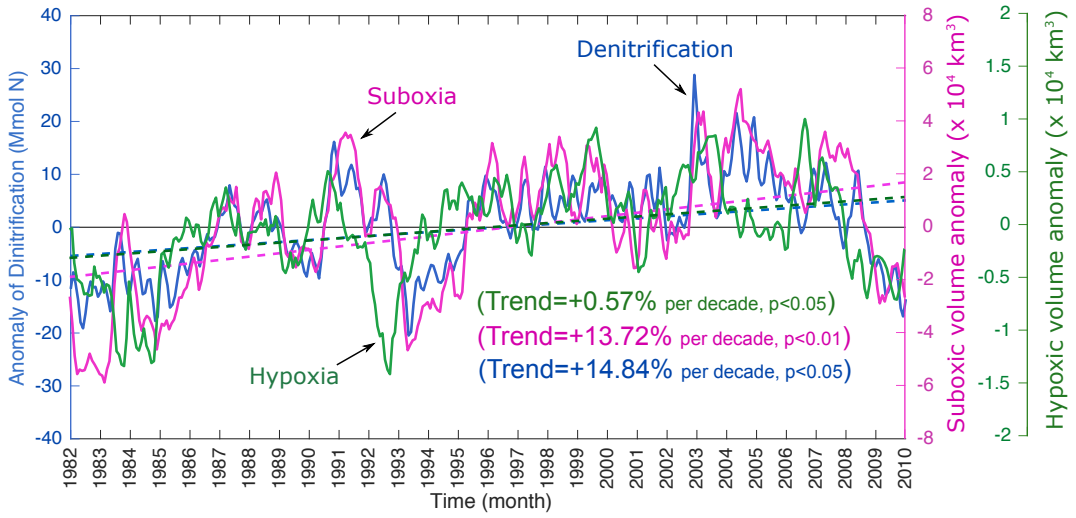

Figure 5. ~~**Changes in Oxygen Minimum Zone intensity and denitrification.**~~ **Changes in Oxygen Minimum Zone and denitrification in northern AS.** Interannual anomalies in the volume of ~~(a)~~ suboxia (~~b~~purple), hypoxia ~~and~~ (~~e~~green) and water column denitrification (blue) in the upper 1000 m north of 20°N over the study period. The dashed lines indicate the trend lines. The location of the northern AS box is shown in Fig 4a.

nearly 100% for suboxia. Next, we focus on the northern AS (north of 20°N) where simulated deoxygenation and its impacts on the OMZ are the most prominent.

3.2 Drivers of northern AS ocean deoxygenation

~~In the~~ As oxygen equilibrates relatively rapidly at the air-sea interface relative to ocean circulation timescales, observed surface oxygen concentrations are generally close to their saturation levels (O_2^{sat}). In the ocean interior, oxygen is depleted because of biological respiration. Therefore, changes in dissolved oxygen concentrations in the ocean interior translate either changes in oxygen saturation levels (solubility effect) or changes in the accumulated oxygen deficits associated with respiration. The latter term, measured by AOU ($AOU=O_2^{sat}-O_2$), depends on both biological activity and ventilation. Here, we explore how these different components contribute to the simulated oxygen changes. In the northern AS (north of 20°N), oxygen inventory drops by ~~nearly 2.2~~over 6% per decade ~~and up to 7% per decade in the upper 200 m and between 200~~ between 100 and 1000 m~~, respectively~~. (Fig. ~~8b and Fig. 8c~~6). We found ~~these trends~~ this trend to be statistically significant at 95% confidence interval~~in both layers. The decline of O_2 near the surface (top 30 m) is weaker in relative terms (-0.35% decade^{-1}) and is predominantly (over 70%) driven by a drop in O_2 saturation associated with decreasing solubility (Fig 8a). Yet, deoxygenation trends in the thermocline (0-200 m) and in the ocean interior (200-1000 m) seem~~. The deoxygenation trend seems to emerge mostly from changes in the apparent oxygen utilization (AOU) as O_2~~saturation declines very weakly in the upper 200 m~~ ^{sat} shows no similar decline and even slightly increases ~~below 200 m~~ during the study period (Fig. ~~8b and Fig. 8c~~) .

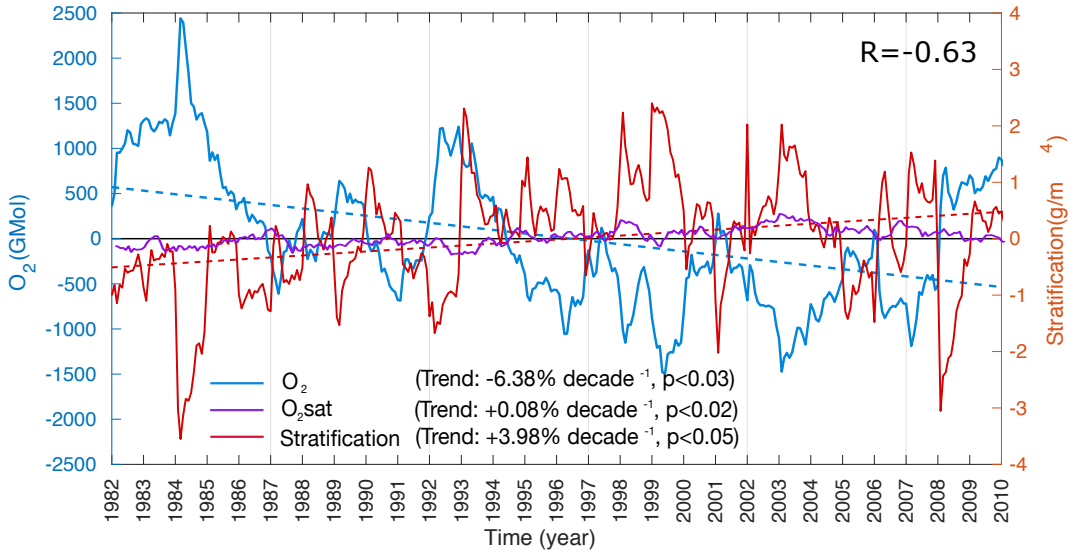

Figure 6. Drivers of northern AS deoxygenation between 1982 and 2010. O_2 content (blue) and O_2 saturation (~~orange~~purple) anomalies ~~in (a) the top 30~~between 100 and 1000 m ~~, (b) the top 200~~and anomalies of vertical stratification at 100 m ~~and~~ (~~e~~red) in the ~~200-1000 m layer~~ northern AS box as a function of time. The blue and red dashed ~~line indicates~~ lines indicate the trend ~~line~~ lines in O_2 inventory and vertical stratification at 100 m (estimated as the local vertical density gradient at 100 m). Note the strong anticorrelation between O_2 anomalies and stratification anomalies (R=-0.63). The location of the northern AS box is shown in ~~each layer~~Fig 4a.

6). This is in contrast to the surface ocean (top 30 m) where the drop in O_2^{sat} explains the majority (over 70%) of the simulated O_2 decline (Fig S19, SI). To further explore the drivers of ocean deoxygenation in the northern AS, we performed an O_2 budget analysis north of 20°N in the ~~100-200~~100-1000 m ~~and the 200-1000 m layers~~ layer (Fig. ~~9~~7). To this end, we quantified ~~the~~ in the same layer the cumulative O_2 anomalies ~~in each of the two vertical layers and calculated the respective contributions of transport and biology to these. In order to explain changes in O_2 that are consistent with the identified linear trends, we run this budget between the first (beginning of 1982) and the last (beginning of 2008) intersection of~~ associated with the transport and the biology sources-minus-sinks terms (see the details of the O_2 ~~time series with the trend line~~mass balance equation in the SI). This analysis indicates that most of O_2 decline in the ~~upper 200 m of the~~ northern region is associated with a drop in ventilation ~~, with little contribution from changes in biological consumption (Fig. 9a). Below 200 m, the increase in biological consumption slightly contributes to the deoxygenation trends, but ventilation reduction still dominates both interannual variability and long-term trends~~ (transport), with O_2 anomalies driven by biological consumption showing no such a drop over the study period (Fig.7). The ventilation anomalies appear to also dominate the strong interannual and decadal variability in O_2 (Fig. ~~9b).~~ 7). The reduction in ventilation in the northern AS is particularly strong in the 1980s and 1990s. In contrast, no such decline can be seen in the last decade of the simulation despite an important modulation by interannual fluctuations. Splitting the ventilation contribution into ~~lateral and vertical components~~ vertical mixing and advection driven parts reveals that the decline in O_2 ~~in the upper 200 m~~ is primarily caused by a reduction in vertical ~~ventilation, whereas below~~

~~200 m deoxygenation is more driven by reduced lateral O_2 supply (Fig S9, SI~~mixing (Fig 7). Next, we explore ~~the changes in physical forcing causing these trends~~how changes in atmospheric forcing may have contributed to the ventilation reduction evidenced by the O_2 budget analysis.

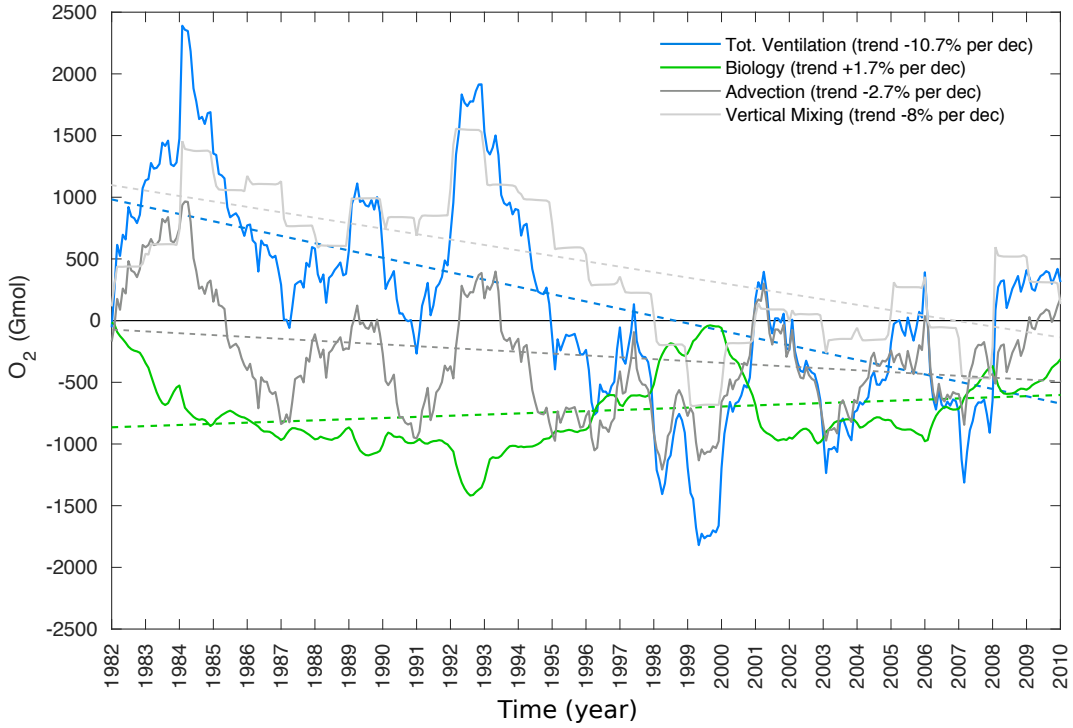

Figure 7. ~~**Role of ventilation and biology in AS deoxygenation.**~~ **Role of ventilation and biology in northern AS deoxygenation.** Cumulative O_2 anomalies associated with ventilation (~~black~~blue) and ~~their~~ biological (green) changes between 100 and ~~physical (blue) sources~~ 1000 m in ~~(c)~~ the northern AS (~~100-200m~~location indicated in Fig 4a)~~subsurface~~. The contributions of advection and ~~(d)~~ subgrid vertical mixing are shown in dark grey and light grey, respectively. The dashed lines indicate the ~~intermediate (200-1000m) ocean~~trend lines associated with the different sources.

3.3 Impact of changes in atmospheric forcing

~~The analysis of long-term trends in atmospheric forcing reveals a widespread warming of the sea surface by between 0.5 and 1°C in the northern AS and by up to 1.5°C in the Gulf and in the northern part of the Red Sea, between 1982 and 2010 (Fig 10a). In addition to surface warming, surface winds have undergone important changes with an intensification of upwelling favorable winds off Somalia and Oman, in particular during the summer monsoon season (Fig 10b and Fig S10, SI).~~

~~**Deoxygenation rates under different atmospheric forcing scenarios.** Linear trends in O_2 inventories (left) in the top 200 m and (right) in the 200-1000 m layer (in % per decade) in the (a-b) S_{hclim} (no warming), (c-d) S_{hclim_AG} (no Gulf warming) and (e-f) S_{wclim_JJAS} (no summer wind changes) simulations. (g-h) Trends in O_2 (in %) in the northern AS (north of 20°N)~~

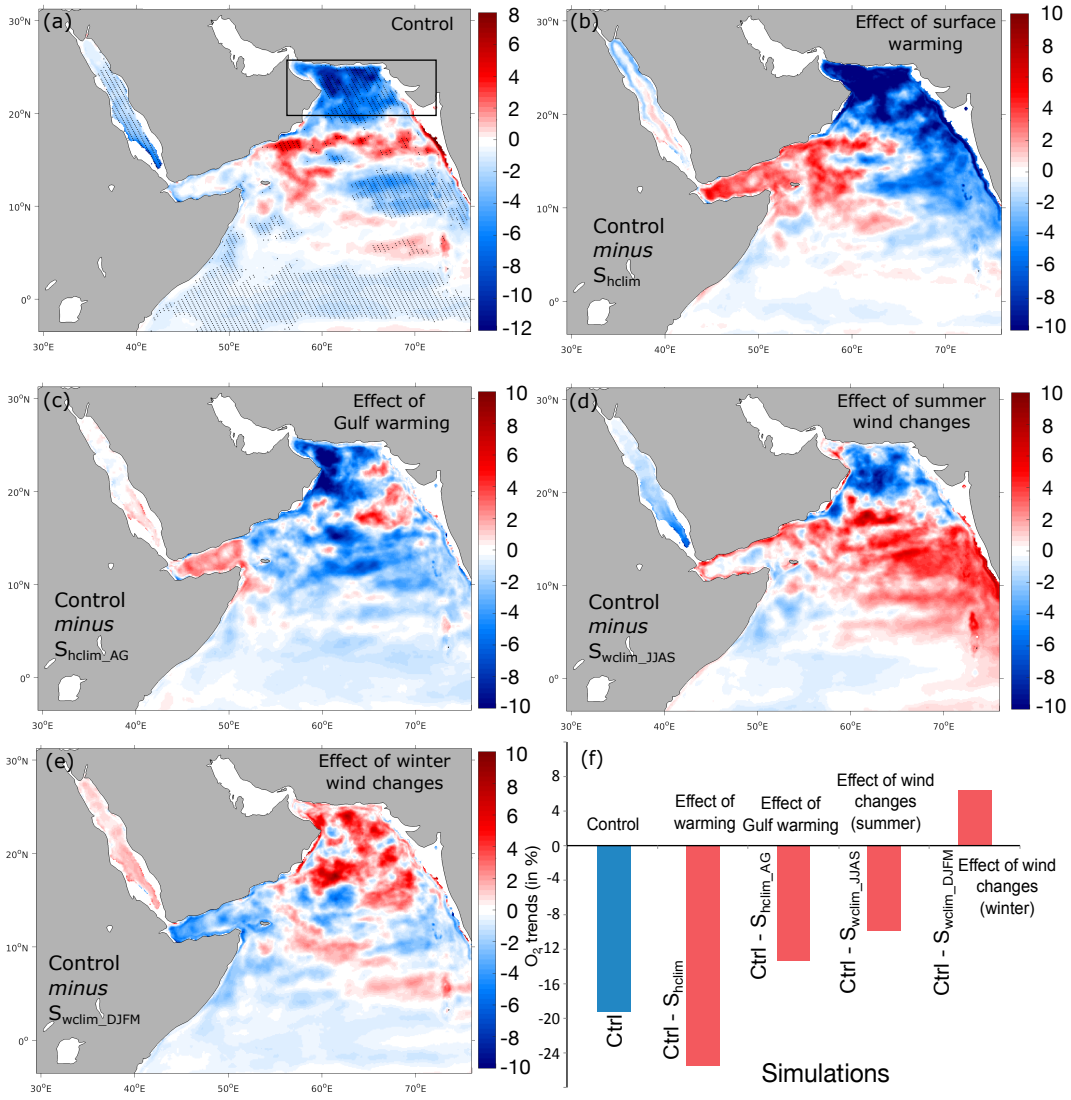

Figure 8. ~~**Warming and surface wind changes.**~~ **Effects of different atmospheric forcing perturbations on deoxygenation rates.** (a) Linear trends in O_2 inventories in the 100-1000 m layer in the control run (~~a) sea surface temperature (~~in ~~°C per~~ % decade^{-1}). (b-e) Difference in O_2 inventory trends between the control run and the S_{hclim} (~~b~~i.e., effect of warming)~~surface winds~~, S_{hclim_AG} (~~color shading indicates trends in~~ i.e., effect of Gulf warming), S_{wclim_JJAS} (i.e., effect of summer wind ~~speed~~ intensification) and S_{wclim_DJFM} (i.e., effect of winter wind changes) sensitivity simulations in ~~m~~the 100-1000 ~~s^{-1}~~ m layer (in % decade^{-1})~~whereas arrows show trends in wind stress vector)~~. ~~Statistically significant~~ (f) Difference in O_2 inventory trends ~~at 95% confidence interval following a Mann-Kendall~~ in the northern AS box between the control and the different sensitivity simulations (~~MK~~in % of the mean O_2 inventory over the 1982-2010 period)~~test are represented by hatching~~.

in the control and under different forcing scenarios in (g) the top 200 m and (h) the 200-1000 m layer. Statistically significant trends at 95% confidence interval following a Mann-Kendall (MK) test are represented by hatching.

To quantify the contributions of surface warming and wind changes to northern AS deoxygenation, we performed three additional sensitivity experiments. In the first simulation, S_{hclim}, all atmospheric and lateral boundary conditions were set to vary interannually like To explore the impacts of changes in atmospheric forcing on the oxygen distribution in the Arabian Sea, we contrast oxygen trends in the control run except the heat fluxes that were extracted from a normal year, 1986, and repeated every year (i.e., climatological heat fluxes). In the second sensitivity run, S_{hclim_AG}, the heat fluxes were similarly extracted from year 1986 and repeated annually, but only over the Gulf region (i. e., climatological heat fluxes over the Gulf only). Finally, in a third simulation Sto trends in the different sensitivity experiments. More concretely, the effect of surface warming on oxygen is quantified by subtracting the trends in the no-warming simulation $S_{welim\_JJAShclim}$ all atmospheric and lateral boundary conditions were set to vary interannually like from those in the control runexcept summer monsoon winds that were extracted from the year 1986 and repeated every year (i. e., climatological summer winds). By comparing S_{hclim} to the control, we can quantify the role of surface warming over the entire domain on deoxygenation. Similarly, contrasting S_{hclim_AG} with . Similarly, subtracting the trends in the no-Gulf-warming simulation S_{hclim_AG} from trends in the control run allows us to measure the relative importance of the fast warming of the Gulf on the deoxygenation in the northern AS. Finally, by comparing S_{wclim_JJAS} to the control we can quantify the role of summer subtracting oxygen trends in the S_{wclim_JJAS} and S_{wclim_DJFM} simulations from the control trends we are able to quantify the effects of summer and winter monsoon wind changesin , respectively, on the simulated deoxygenation.

Under climatological heat fluxes, oxygen increases in most of the AS in This analysis reveals that surface warming causes a substantial decline in the upper 200 m, with the oxygen inventory northern AS oxygen inventory of nearly 25% in the 100-1000m layer between 1982 and 2010 relative to the no warming case (Fig. 8). Indeed, oxygen inventory increased north of 20°N increasing by nearly 1.6by over 6% between 1982 and 2010 (Fig 11). Below 200 m, O_2 strongly increases in the northern AS by nearly 7% over the study under climatological heat fluxes as opposed to a decrease of over 18% in the control run during the same period (Fig 11S20, SI). Contrasting these oxygenation trends with the strong deoxygenation oxygen trends in the no-Gulf warming simulation to those simulated in the control suggests that surface warming is the main cause of deoxygenation in the northern AS (Fig S11, SI). When the heat fluxes are set to be climatological over the Gulf region only, oxygen decreases in run suggests that the northern AS both in the top 200 m and between 200 and 1000 m, but deoxygenation rates are nearly twice (0-200 m) to five times (200-1000 m) weaker than in the control (Fig11 and Fig S11, SI). This indicates that the fast warming over the Gulf has likely contributed to the northern AS recent strong deoxygenation. Finally, in fast warming of the absence of interannual changes in summer winds, simulated deoxygenation rates in Gulf has significantly contributed to northern AS deoxygenation. Concretely, the Gulf warming is associated with a decrease of the northern AS are weaker than in the control simulation (Fig 11). However, deoxygenation trends become stronger in most of the rest of the AS in oxygen inventory of around 12% in the 100-1000m layer between 1982 and 2010 relative to the top 200 m and no-Gulf warming case (Fig. 8). Indeed, in the absence of Gulf warming the oxygen inventory decreased north of 20°N by only around 6% between 1982 and 2010, a rate that is twice as weak as that simulated in the control run during the same period (Fig S20,

SI). The intensification of summer monsoon winds also appears to contribute to simulated deoxygenation in the ~~central and eastern AS below 200 m (Fig 11 and Fig S11~~northern AS, although to a lesser extent (Fig 8). Indeed, summer wind changes are associated with a decrease of the northern AS oxygen inventory of around 9% in the 100-1000m layer between 1982 and 2010 relative to the no summer wind change scenario (Fig 8). This is as oxygen decreases in the northern AS by around 9% between 1982 and 2010 under climatological summer winds, a rate that is nearly 50% weaker than in the control run during the same period (Fig S20, SI). ~~This suggests that summer upwelling intensificationcontributes to deoxygenation~~ Finally, contrary to surface warming and summer monsoon intensification, changes in winter monsoon winds do not contribute to deoxygenation trends in the northern ~~AS and in the western AS at depth but acts to oxygenate the upper ocean in the rest of the AS~~ Arabian Sea. Indeed, in the absence of winter wind changes, deoxygenation in the northern AS is maintained and is even slightly stronger relative to the control run (Fig 7).

In summary, we conclude that deoxygenation in the northern AS is essentially caused by surface warming and that the fast warming of the Gulf plays an important role in this trend. ~~Summer monsoon intensification~~ While summer monsoon intensification - to a lesser extent- contributes to deoxygenation in the northern AS~~as well as in the western AS at depth. However, increasing summer winds do also enhance the oxygenation of the upper ocean south of 20°N.~~ , changes in winter monsoon winds have a smaller effect on northern AS oxygen and tends to oppose deoxygenation trends there. Next, we explore the mechanisms through which surface warming and enhanced summer monsoon winds ~~cause these oxygen trends~~reduce thermocline ventilation, causing upper ocean deoxygenation in the northern AS.

3.4 Mechanisms of ~~Arabian sea reduced~~ ventilation reduction

The ~~strong surface warming resulted~~ ventilation of the northern AS upper thermocline is predominantly sensitive to: (i) the intensity of vertical mixing particularly associated with winter convection (McCreary et al., 2013; Resplandy et al., 2012) , (ii) the magnitude of export and subduction of dense Gulf water (Lachkar et al., 2019) and (iii) the vertical displacement of the thermocline causing changes in the oxycline depth (Vallivattathillam et al., 2017). Here, we explore how these ventilation mechanisms have responded to changes in atmospheric forcing.

The ocean surface warming results in an increase in vertical stratification (here estimated using the local vertical density gradient at 100 m) that is particularly important in the northern AS with stratification at ~~200~~100 m increasing on average by nearly 4% per decade ~~(Fig 12a and Fig S12a, SI~~north of 20°N (Fig 6 and Fig 9). This ~~likely contributes to the reduction in the vertical ventilation in the upper ocean as revealed by our O_2 budget analysis (Fig S9, SI). Under climatological heat fluxes, upper ocean stratification does decrease in most of the AS, and in particular in the northern AS (Fig 12c and Fig S12~~positive trend is mostly induced by rapid stratification increases in the 1980s and 1990s with little change in the 2000s, mirroring the evolution of O_2 (Fig 6). The stratification does not increase (even slightly decreases) in the northern AS when the heat fluxes are set to be climatological (Fig S21, SI). This confirms that ~~most of the increase in vertical stratification in the control simulation is caused by surface warming (Fig S13a, SI).~~

~~When the heat fluxes are set to be climatological over the Gulf only, the increase in vertical stratification is similar to that in the control run over most of the AS , including the region north of 20°N (Fig S12 and Fig S12~~surface warming is responsible

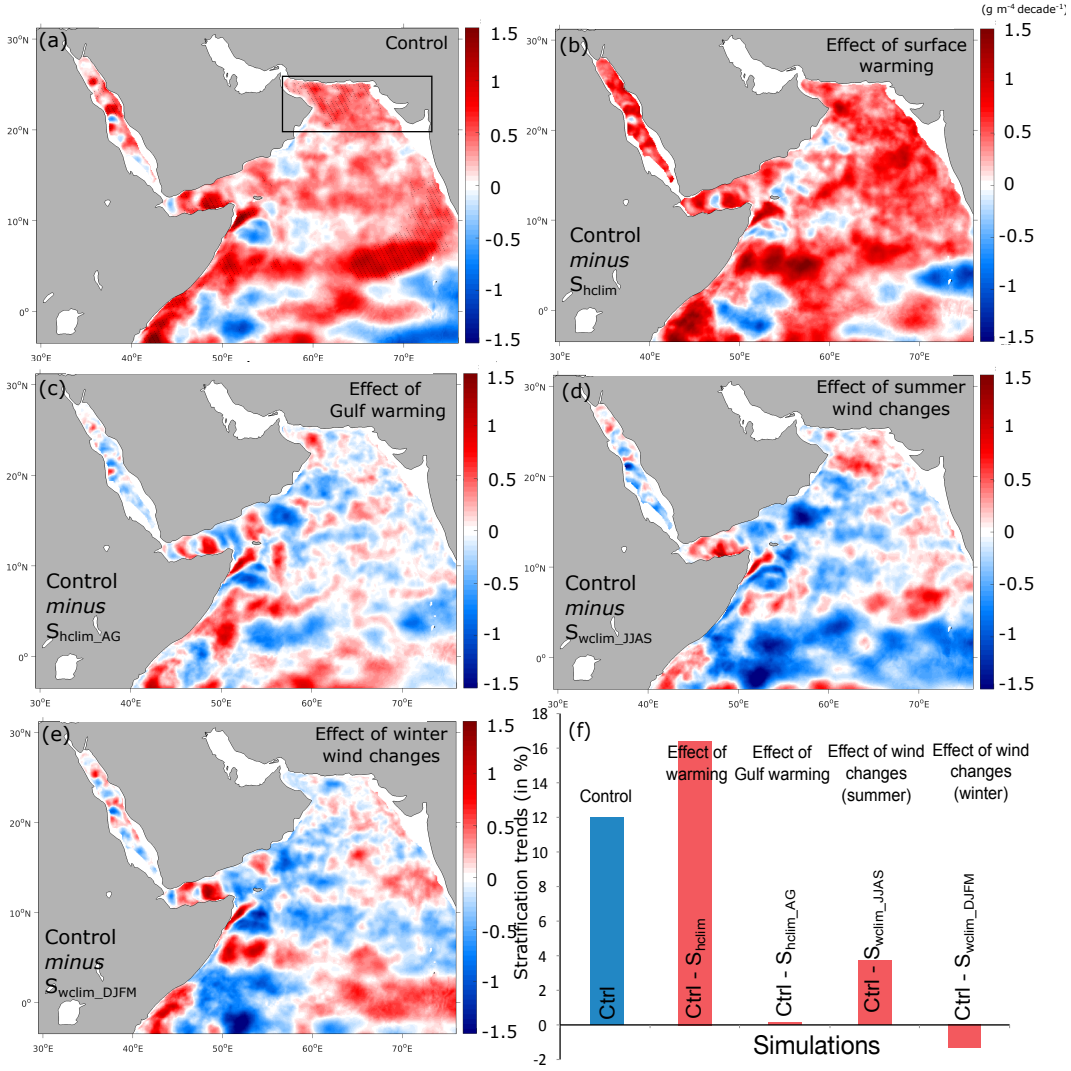

Figure 9. ~~Vertical stratification and thermocline depth under different atmospheric forcing scenarios.~~ **Effects of different atmospheric forcing perturbations on upper ocean vertical stratification.** (a) Linear trends in ~~(left)~~ vertical stratification at 100 m in the control run (in g m^{-4} decade^{-1}). (b-e) Difference in trends in stratification at 100 m between the control run and the S_{hclim} (~~right~~i.e., effect of warming)~~depth~~, S_{hclim_AG} (i.e., effect of ~~isotherm 20°C D20~~ Gulf warming), S_{wclim_JJAS} (i.e., effect of summer wind intensification) and S_{wclim_DJFM} (i.e., effect of winter wind changes) sensitivity simulations (in g m^{-4} decade^{-1})~~in the~~. (~~a-b~~f) Difference in stratification trends in the northern AS box between the control and ~~(c-h) under~~ the different ~~atmospheric forcing scenarios. Statistically significant trends at 95% confidence interval following a Mann-Kendall~~ sensitivity simulations (~~MK~~in % of the mean stratification over the 1982-2010 period)~~test are represented by hatching~~.

for the stratification increase that inhibits vertical mixing and contributes to the reduction of ventilation revealed by the O_2 budget analysis (Fig 7). Additional evidence for the reduced vertical mixing can be seen from the analysis of trends in winter

mixed layer depth (MLD) that shows a winter MLD shoaling by over 5 m in the northern AS between 1982 and 2010 (Fig S22, SI). ~~This suggests that the reduction in the ventilation of the northern AS is not entirely caused by enhanced vertical stratification and~~

While both the warming of the Gulf and summer monsoon intensification contribute to deoxygenation in the northern AS, vertical stratification changes little in response to these two perturbations (Fig 9 and Fig S21). This suggests that other mechanisms ~~are likely at play~~contribute to northern AS ventilation reduction besides vertical stratification enhancement. Lachkar et al. (2019) have shown that the AS OMZ can intensify in response to strong warming of the Gulf causing a reduced outflow of the Gulf water in the northern AS. Here, we find the depth of the Gulf water has shoaled locally by up to 20 m in the Gulf of Oman in the control run relative to the S_{hclim_AG} run (Fig ~~S14~~S23, SI). This indicates an increase in the Gulf water buoyancy and a decline in its subduction to intermediate depths in the northern AS in agreement with the mechanisms described in Lachkar et al. (2019).

Finally, ~~the summer monsoon wind intensification is~~ changes in monsoon winds are likely to affect ~~upper ocean mixing and thermocline depth, and hence vertical ventilation and~~ oxygen levels in the upper ocean ~~. Furthermore, changes in summer monsoon winds can also affect upwelling off Somalia and Oman and hence alter productivity and O_2 consumption at depth in the western AS, potentially impacting O_2 supply to northern AS. The analysis of~~ through their impact on the thermocline depth, and hence the depth of the oxycline. Here we analyze long-term trends in thermocline depth, ~~typically~~ noted D20 and represented by the depth of isotherm 20°C ~~in the tropical Indian Ocean (e.g. Schott et al., 2009),~~ following previous studies (e.g. Schott et al., 2009). This analysis reveals a shoaling of this interface ~~in the western and northern AS by up to~~ by over 3% (around 6 m~~per decade and a slight deepening in the central and eastern AS (Fig 12b). In contrast~~) in the northern AS between 1982 and 2010 (Fig 10). Contrasting these trends to those simulated under climatological summer winds shows a strong sensitivity of this parameter to summer monsoon wind intensification. Indeed, under climatological summer monsoon winds the ~~themocline depth~~ thermocline depth D20 shoals almost everywhere in the AS except in the northern region where a deepening is ~~observed (Fig 12h~~simulated (Fig S21, SI). This suggests that summer monsoon wind intensification ~~cause~~ causes the thermocline depth to rise in the northern AS and deepen elsewhere (Fig ~~S15c, SI~~10). The shoaling of the thermocline depth contributes to lowering O_2 levels in the ~~upper 200 m in the northern AS~~ northern AS upper thermocline whereas its deepening south of 20°N contributes to ~~increase O_2 levels in the top 200 m. Increased summer monsoon winds increase biological productivity in the western and central AS by up to 5% per decade in the control run (Fig 13). In contrast, productivity shows a limited increase or even a decrease in the western AS under climatological summer winds (Fig 13). The enhancement in productivity south of 20°N that results from summer monsoon wind intensification is associated with an increase in O_2 consumption (hence a decrease in O_2) at depth in the central and western AS (Fig S16c and Fig S17c~~oxygenate the upper ocean there. This analysis also shows that changes in winter monsoon winds are associated with a deepening of the thermocline in the northern AS (potentially linked to enhanced downwelling along the west coast of India) that contributes to oxygenate the upper thermocline (Fig 2, Fig 10 and Fig S17, SI). ~~This contributes to deoxygenation observed at depth in the central and western AS . The lower O_2 levels in the central and western AS are likely contributing to the reduced~~

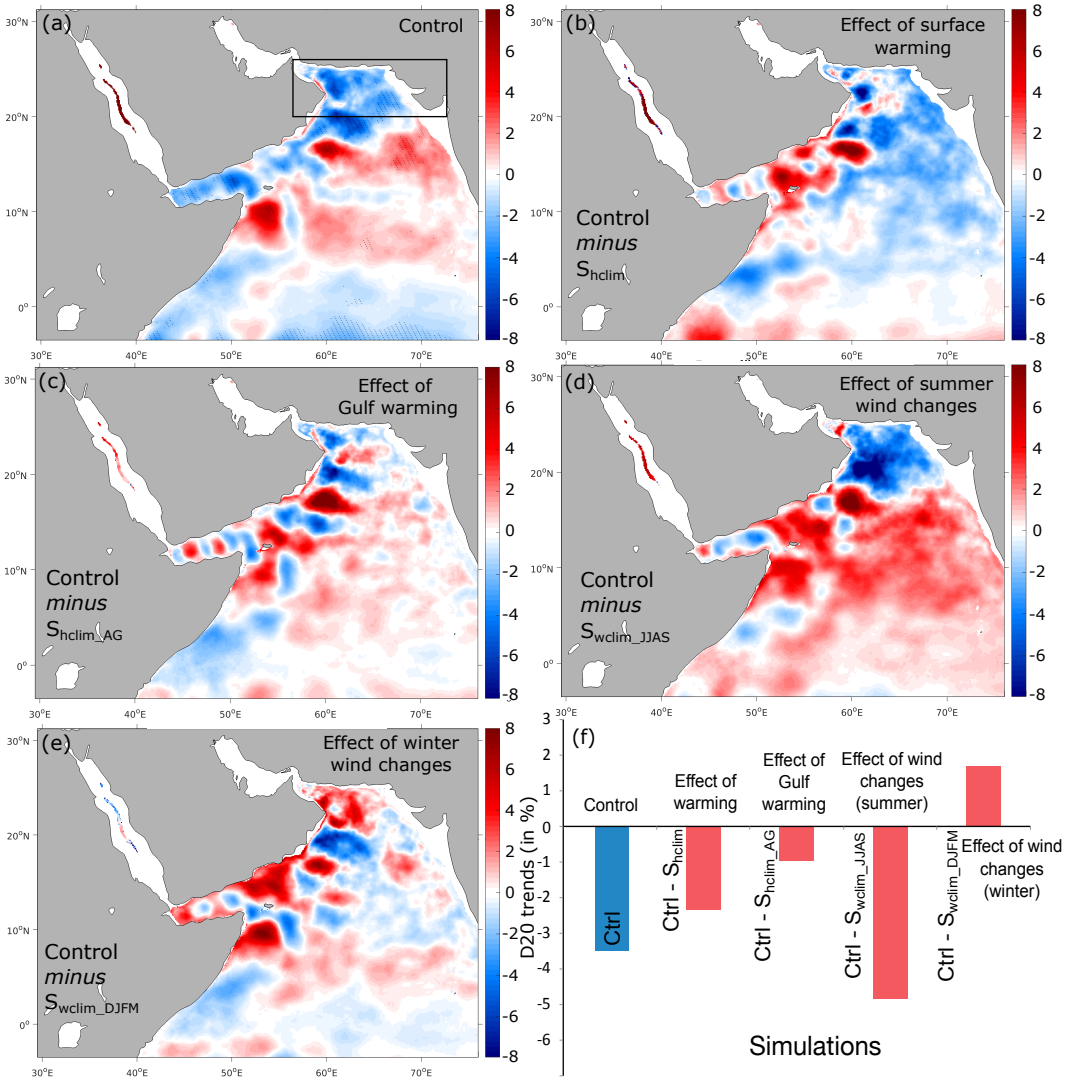

Figure 10. ~~**Net primary productivity and O_2 changes due to remineralization under different atmospheric forcing scenarios.**~~ **Effects of different atmospheric forcing perturbations on thermocline depth.** (a) Linear trends in the depth of isotherm 20°C (~~left~~D20) ~~NPP~~ in the control run (in ~~mol~~ m $^{-2}$ ~~yr^{-1}~~ decade^{-1})~~and~~ . (~~right~~b-e) ~~O_2 changes due to organic matter remineralization~~ Difference in D20 trends between the ~~200-1000 m layer~~ control run and the S_{hclim} (i.e., effect of warming), S_{hclim_AG} (i.e., effect of Gulf warming), S_{wclim_JJAS} (i.e., effect of summer wind intensification) and S_{wclim_DJFM} (i.e., effect of winter wind changes) sensitivity simulations (in ~~mmol~~ m $^{-2}$ ~~s^{-1}~~ decade^{-1})~~in the~~ . (~~a-b~~f) Difference in D20 trends in the northern AS box between the control and ~~(c-h) under~~ the different ~~atmospheric forcing scenatios. Statistically significant trends at 95% confidence interval following a Mann-Kendall~~ sensitivity simulations (~~MK~~in % of the mean thermocline depth over the 1982-2010 period)~~test are represented by hatching~~..

In summary, the analysis of the sensitivity simulations suggests that recent deoxygenation in the northern AS has essentially been caused by surface warming, increasing stratification and inhibiting convective vertical mixing as well as increasing the buoyancy of the Gulf water, thus inhibiting its subduction to intermediate depths. The concomitant shoaling of the thermocline in the northern AS driven by summer monsoon wind intensification further contributes to lower O_2 ~~supply to the northern AS (Fig S9b, SI) as meridional circulation shows little change over the study period (Fig S18, SI~~in the upper ocean there (See Fig 11 for a visual depiction of the key mechanisms involved in northern AS recent deoxygenation).

4 Discussion

4.1 Role of biology

The relatively limited role of biology in the northern AS deoxygenation is a direct consequence of the minimal change the biological productivity has experienced in the region over the study period as well as due to the negative feedback of enhanced denitrification on O_2 consumption at depth. Indeed, the biological productivity has changed little in the northern AS as enhanced stratification on the one hand and increased summer upwelling on the other hand have opposing effects on nutrient supply to the euphotic zone (Fig 12). For instance, productivity increases substantially in the northern AS and across the domain in the absence of surface warming (Fig ~~13~~S24, SI). Conversely, under climatological summer winds productivity tends to decrease in most of the northern and western AS (Fig ~~13~~S24, SI). Finally, the enhanced denitrification associated with the deoxygenation trends reduces aerobic O_2 consumption and hence opposes deoxygenation in the northern AS (Fig ~~S19~~S26, SI). However, biology appears to play a more important role in the central and western AS as increased summer monsoon winds increase the productivity there (Fig 12 and Fig S24, SI). This productivity enhancement results in an increase in O_2 consumption that contributes to the simulated deoxygenation trends in these regions (Fig S24 and Fig S25, SI).

4.2 Comparison with previous works

~~The fact that recent subsurface deoxygenation in the northern AS has been mostly driven by reduced ventilation is consistent with previous results from Earth System models showing that tropical subsurface ocean O_2 changes projected for the twenty-first century and those simulated during the last deglaciation are more driven by changes in ventilation than biology (Bopp et al., 2017) . Our analysis has revealed that summer monsoon wind increase over the study period has mostly caused upper ocean oxygenation (south of 20°N),~~ Roxy et al. (2016) have reported a decline in surface chlorophyll-a over the northern and western AS between 1998 and ~~to a lesser extent has contributed to deoxygenation at depth (through enhanced O_2 consumption). This is consistent with the findings of Lachkar et al. (2018) who investigated the impacts of idealized perturbations in monsoon wind intensity on the size and intensity of~~ 2013. This appears to be inconsistent with results from the present study that show very weak NPP trends in the northern AS and even a statistically significant increase in the western Arabian Sea off the coast of Somalia. There are two main differences between our study and the work of Roxy et al. (2016) that may explain this apparent inconsistency. First, in their analysis Roxy and colleagues have considered surface chlorophyll while we are analyzing trends in vertically

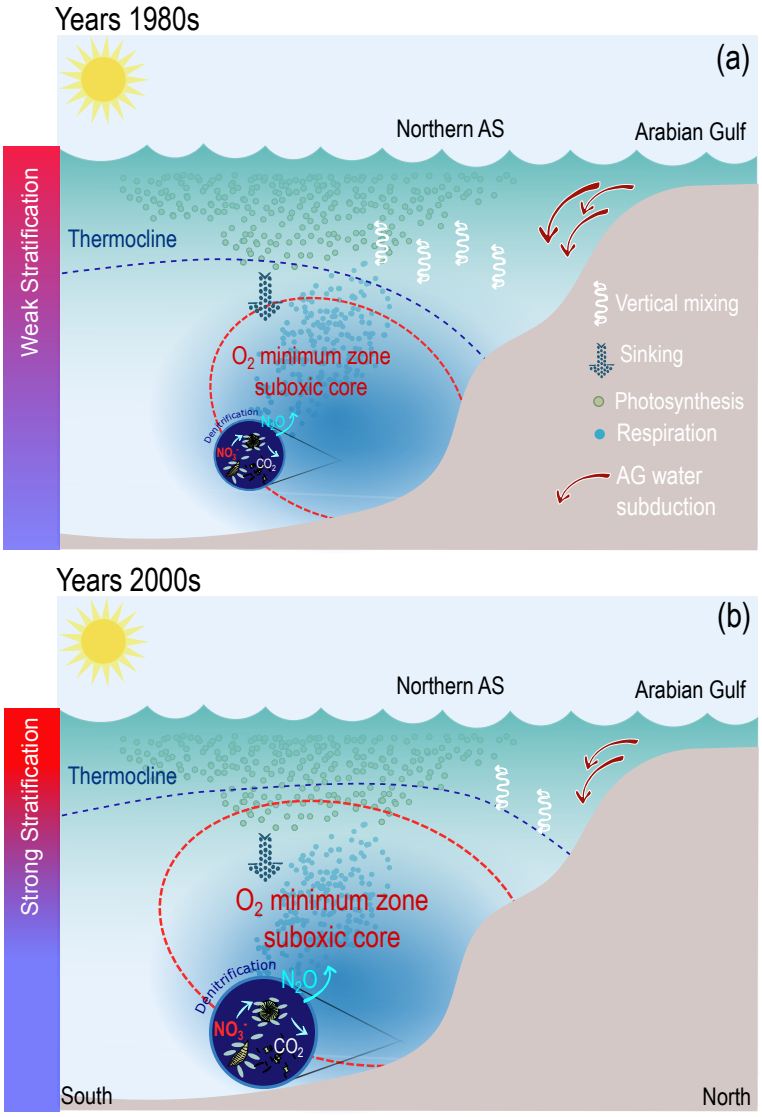

Figure 11. **A schematic summarizing the main processes responsible for the O_2 changes in the northern AS.** (a) Conditions in the early 1980s: cool conditions favor weak stratification, enhanced vertical mixing as well as subduction of high-density Gulf water in the northern Arabian Sea, resulting in a deeper and smaller OMZ suboxic core. (b) Conditions in the early 2000s: warm conditions enhance vertical stratification and cause a weaker vertical mixing and a reduced subduction of the Gulf water in the northern Arabian, resulting in an expansion of the suboxic core of the OMZ and an increase in denitrification. Stronger upwelling favorable winds also contribute to raise the thermocline depth and hence bring O_2-depleted waters upwards further near the surface.

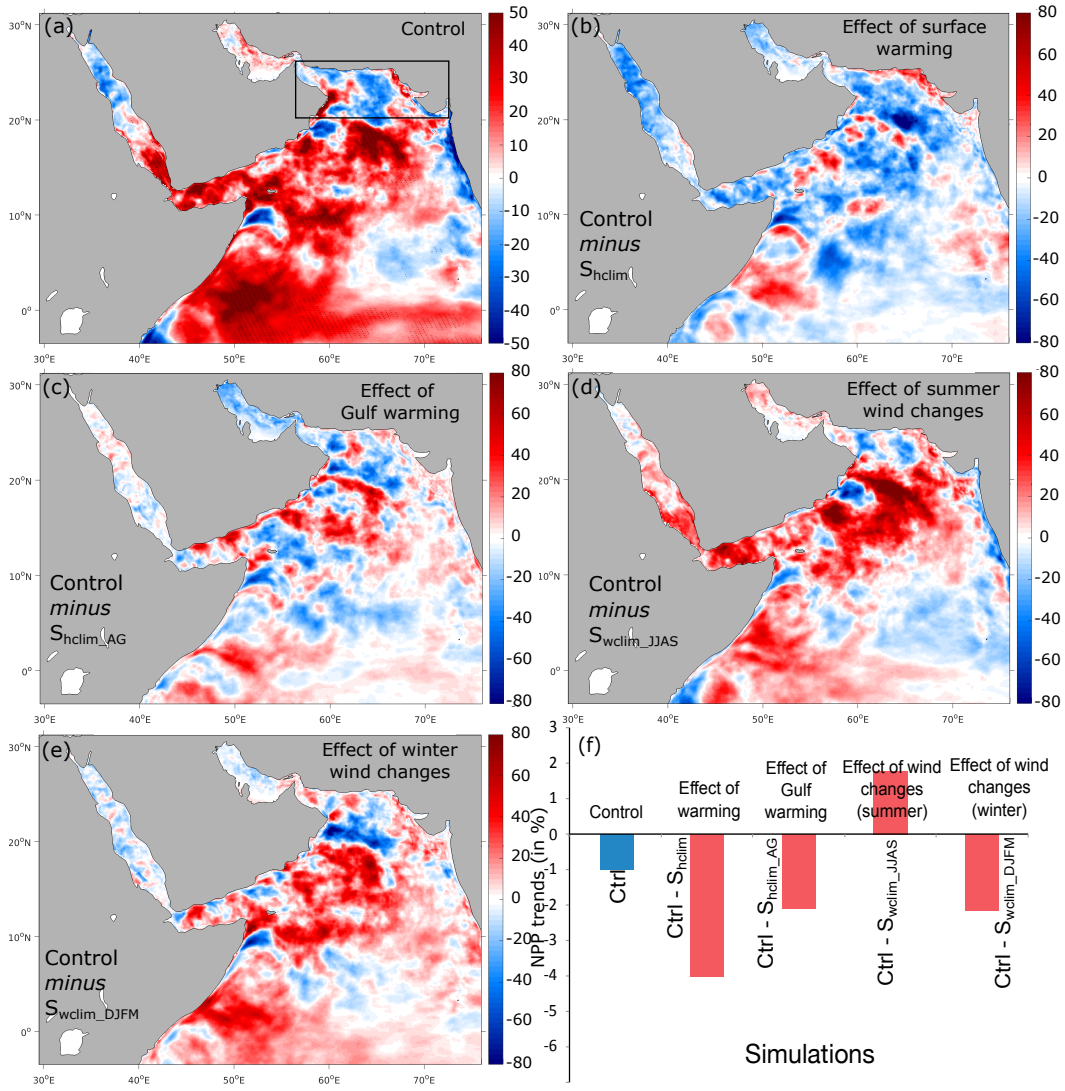

Figure 12. Effects of different atmospheric forcing perturbations on net primary production (NPP). (a) Linear trends in NPP in the control run (in mol m^{-2} yr^{-1} $decade^{-1}$). (b-e) Difference in NPP trends between the control run and the S_{hclim} (i.e., effect of warming), S_{hclim_AG} (i.e., effect of Gulf warming), S_{wclim_JJAS} (i.e., effect of summer wind intensification) and S_{wclim_DJFM} (i.e., effect of winter wind changes) sensitivity simulations (in mol m^{-2} yr^{-1} $decade^{-1}$). (f) Difference in NPP trends in the northern AS box between the control and the different sensitivity simulations (in % of the mean NPP over the 1982-2010 period)..

integrated biological productivity. While these two quantities are usually strongly correlated, they are not identical, especially in tropical systems where deep chlorophyll maxima are commonly observed. Indeed, the trends in surface chlorophyll in our simulation are quite different and are much weaker in the open ocean in comparison to trends in NPP (Fig S27, SI). The second main difference concerns the study periods. Indeed, the satellite chlorophyll data presented in Roxy et al. (2016) is based on

a different and shorter period (1998-2013) than in the present study (1982-2010). Interestingly, our model also simulates a decline of surface chlorophyll in the western Arabian Sea when the analysis is restricted to the period between 1998 and 2010 (Fig S27, SI). We believe the high sensitivity of the ~~AS OMZ and found that the OMZ expands and deepens in response to monsoon wind intensification.~~ trends to the considered period of analysis is an indicator of the strong interannual and decadal variability in the region. This can also be seen in chlorophyll trends based on CMIP models presented in Roxy et al. (2016) . Indeed, covering a longer period (1950-2005) these time series reveal strong decadal variability with a decline in surface chlorophyll from the 1950s to the late 1970s followed by no significant trend or even a slight increase over the period from 1980 and 2005.

Our finding that the suboxic volume and denitrification are highly sensitive to deoxygenation is consistent with previous studies that suggest high vulnerability of suboxic zones to small changes in the ocean's O_2 content. For instance, the world's largest suboxic zone in the Pacific Ocean was shown to vary in size by a factor two in ~~model-based~~ model reconstructions of historical oxygen changes (Deutsch et al., 2011). Finally, the weaker sensitivity of the volume of hypoxia to ~~deoxygneation~~ deoxygenation in the AS is ~~a consequence of the near compensation by wind-driven oxygenation trends in the central and eastern AS and is~~ consistent with previous studies suggesting a generally weaker sensitivity of the hypoxic volume to deoxygenation. For instance, it was estimated that a decrease of the upper ocean O_2 concentration by 5 mmol m^{-3} could lead to a tripling of the suboxic volume and only 10% increase in the hypoxic volume (Deutsch et al., 2011).

4.3 Future deoxygenation in the northern AS

As the AS and the Gulf continue to warm under future climate change, deoxygenation may ~~accelerate in the region. Modeling studies suggest indeed further~~ continue in the northern AS region. Indeed, modeling studies suggest further future ocean deoxygenation in the ~~northern AS in the future~~region. For instance, CMIP5 models project a drop of O_2 by up to 20 mmol m^{-3} in the Sea of Oman in the layer between 200 m and 600 m by the end of the century under the RCP8.5 emission scenario (Bopp et al., 2013). The CMIP6 multi-model ensemble average indicates an even stronger oxygen decline of more than 30 mmol m^{-3} by 2100, in the northern AS between 100 m and 600 m, essentially driven by an increase in the AOU (Kwiatkowski et al., 2020). These changes can have dramatic impacts on O_2-sensitive species and nitrogen and carbon cycling in the region. Furthermore, the impacts of these O_2 changes on marine ecosystems are likely to be exacerbated by concurrent stressors such as warming, declining productivity and ocean acidification ~~. For instance, the fast warming of the ASupper ocean is likely to cause an increase in the metabolic rates. This in turn is expected to increase organisms oxygen demand at the same time where O_2 supply to the environment is dropping (Levin, 2018; Deutsch et al., 2015). Furthermore, oxygen-induced vertical plankton migration can intensify~~ (Levin, 2018; Deutsch et al., 2015; Gobler and Baumann, 2016; Miller et al., 2016; Bianchi et al., 2013). In the central and southern AS, however, global model projections show no consistent trends or even a slight oxygenation (Bopp et al., 2013; Kwia . This may be due to the relatively important future productivity decline these models predict for the western and central AS that may reduce O_2 ~~depletion at depth (Bianchi et al., 2013). It is also established that ocean acidification interacts with deoxygenation and can aggravate the effects of low oxygen on organisms (Gobler and Baumann, 2016; Miller et al., 2016)~~ consumption there and compensate for the effect of reduced ventilation.

4.4 Caveats and limitations

Our study has a couple of caveats and limitations. Among the study's main limitations is the relatively short simulation period that precludes the attribution of the documented O_2 changes to climate change vs. natural variability. Previous observations suggest that the natural variability in O_2, dominated by interannual and decadal oscillations, can locally be stronger than the long-term trends associated with climate warming (Whitney et al., 2007; Cummins and Ross, 2020). Strong modulation of interrannual variability in hypoxic and suboxic volumes by decadal oscillations has been documented in previous studies (e.g., Deutsch et al., 2011, 2014). This complicates the detection and attribution of long-term responses to climate change ~~.~~ (Bindoff et al., 2019). Therefore, it is ~~not unlikely~~ possible that an important fraction of the trends simulated here is associated with natural variability as it has been shown that the emergence of the climate change signal among the internal variability range is generally slow for oxygen, with only a small fraction of the ocean experiencing emergence before the end of the century (Frölicher et al., 2016). According to the same study, the earliest emergence of the O_2 signal in the AS is expected to occur only by the middle of the current century~~. Yet,~~ , although this may also happen significantly earlier according to other studies ~~the emergence of the climate change signal from the noise of natural variability can occur as early as 2010 or 2020 in the ventilated thermocline of the northern AS~~ (Long et al., 2016; Hameau et al., 2019).

An additional caveat of the study is related to the uncertainty around the recent monsoon wind changes. Indeed, no clear consensus emerges from the different studies that have explored the recent and future wind changes in the region, as some point to an intensification (e.g., Wang et al., 2013) whereas others suggest a weakening (e.g., Swapna et al., 2017) or a poleward shift (e.g., Sandeep and Ajayamohan, 2015). Some of this uncertainty may be associated with the strong decadal variability that modulates the surface winds in the region and may lead to aliasing of long-term trends. An additional source of uncertainty is the lack of observations in the AS region that results in not very well constrained reanalyses. To test this, we contrast the trends in surface winds estimated over the study period (1982-2010) from three reanalysis products: ERA-Interim (here used to force the model), the National Centers for Environmental Prediction reanalysis II (NCEP-2) and the Japanese 55-year Reanalysis Project (JRA-55). This comparison reveals important discrepancies among the three products (Fig S28, SI). Indeed, while the NCEP2 winds show a modest increase in upwelling-favorable winds in the western Arabian Sea, there seems to be no such an increase (and even a slight weakening) in the JRA55 winds. While we acknowledge this uncertainty as one of the caveats of the study, we also believe this has likely limited implications for the conclusions of the study as we demonstrate here that surface warming is the dominant factor in the northern Arabian Sea deoxygenation, with the surface wind changes playing only a secondary role.

Other study limitations pertain to the biogeochemical model assumptions and model forcing. For instance, the lack of a representation of some major limiting nutrients such as iron, silicate and phosphate can potentially cause biases in regions where these nutrients contribute to limit biological production (e.g., off Somalia). However, previous studies suggest nitrogen is the main limiting nutrient in the Indian Ocean at larger scales (Koné et al., 2009). Other major model-related limitations concern the lack of representation of important biogeochemical processes such as N_2 fixation and the crude representation of microbial respiration in the model. Yet, on the one hand recent studies suggest that N_2 fixation has a limited effect on the AS OMZ as it

constitutes only a negligible proportion of new nitrogen there (Guieu et al., 2019). On the other hand, simple representations of microbial respiration that miss potentially important biogeochemical ~~feedbacks~~ feedback are a common problem in most existing biogeochemical models (Oschlies et al., 2018; Robinson, 2019). Additional work that ~~combine~~ combines expanding the current oxygen-measurement system and improving the complexity of microbial respiration in numerical models is needed to reduce biases in model estimates of deoxygenation (Oschlies et al., 2018). Finally, as the model lateral boundary conditions for nitrate and oxygen were set to be climatological, the effects of potential changes in either O_2 or NO_3^- at the domain southern boundary at 31°S are not taken into account. Previous studies (e.g., Keller et al., 2016; Fu et al., 2018) have shown that remote biological processes in the Southern Ocean can significantly affect oxygen levels and OMZs in the tropics either through trapping of nutrients in the Southern Ocean or through changes in O_2 levels of locally formed mode and intermediate waters. However, these remote influences have been shown to affect oxygen in the tropics (including the Arabian Sea OMZ region) only on timescales of several decades to centuries (Keller et al., 2016). Therefore, given the short time period considered in the present study we believe the lack of interannual variability at the domain lateral boundaries to have limited impact on our results.

5 Summary and Conclusions

We reconstruct the evolution of dissolved ~~ocean~~ oxygen in the AS from 1982 through 2010 using a series of hindcast simulations performed with an eddy-resolving ocean biogeochemical model forced with ~~ERA~~ ERA-Interim atmospheric reanalysis. We find a significant thermocline deoxygenation in the northern ~~and western~~ AS, with the ocean O_2 content dropping by ~~around~~ ~~2~~over 6% decade^{-1} ~~and 7% decade^{-1} in the 0-200~~in the 100-1000 m ~~and the 200-1000 m, respectively~~layer. These changes are ~~associated with~~ accompanied by a statistically significant increase of the volume of suboxia (O_2 < ~~4mmol~~4 mmol m^{-3}) and denitrification by up to 30% ~~around~~ and 40% over the study period, respectively. Using a set of sensitivity simulations we demonstrate that deoxygenation in the northern AS has been caused essentially by a widespread warming of the sea surface, in particular in the Gulf, causing a reduction in the ventilation of the subsurface and intermediate layers. Additionally, we show that a concomitant summer monsoon intensification over the study period has enhanced the ventilation and hence the oxygenation of the upper ocean south of 20°N but has contributed to deoxygenation in the northern AS~~and at depth~~. This is because ~~surface warming~~ on the one hand surface warming: (i) increases vertical stratification, thus reducing ~~ventilation of the intermediate ocean, while~~ vertical mixing and (ii) increases the Gulf water buoyancy, inhibiting its subduction to intermediate depths. On the other hand, summer monsoon wind intensification causes the thermocline depth to rise in the northern AS and deepen elsewhere, thus contributing to lowering O_2 levels in the upper ~~200 m in the northern AS~~ layers north of 20°N and increasing it in the rest of the ~~AS. Finally, wind change-driven enhanced productivity south of 20°N contributes to deoxygenation observed at depth in the western and central~~ AS. Our findings confirm that the AS OMZ is strongly sensitive to upper-ocean warming and concurrent changes in the Indian monsoon winds. Our results also demonstrate that changes in the local climatic forcing play a key role in regional dissolved oxygen changes and hence need to be properly represented in global models to reduce uncertainties in future projections of deoxygenation.

Acknowledgements. Support for this research has come from the Center for Prototype Climate Modeling (CPCM), the New York University Abu Dhabi (NYUAD) Research Institute. Computations were performed at the High Performance cluster (HPC) of NYUAD, Dalma. We thank B. Marchand and M. Barwani from the NYUAD HPC team for technical support. The authors declare that they have no competing financial interests. The data used for forcing and validating the model are publicly available online and can be accessed from cited references.

The model code can be accessed online at http://www.romsagrif.org.

References

Al-Ansari, E. M., Rowe, G., Abdel-Moati, M., Yigiterhan, O., Al-Maslamani, I., Al-Yafei, M., Al-Shaikh, I., and Upstill-Goddard, R.: Hypoxia in the central Arabian Gulf Exclusive Economic Zone (EEZ) of Qatar during summer season, Estuarine, Coastal and Shelf Science, 159, 60–68, 2015.

Al-Rashidi, T. B., El-Gamily, H. I., Amos, C. L., and Rakha, K. A.: Sea surface temperature trends in Kuwait bay, Arabian Gulf, Natural Hazards, 50, 73–82, 2009.

Al-Yamani, F. and Naqvi, S.: Chemical oceanography of the Arabian Gulf, Deep Sea Research Part II: Topical Studies in Oceanography, 161, 72–80, 2019.

Bange, H. W., Naqvi, S. W. A., and Codispoti, L.: The nitrogen cycle in the Arabian Sea, Progress in Oceanography, 65, 145–158, 2005.

Banse, K., Naqvi, S., Narvekar, P., Postel, J., and Jayakumar, D.: Oxygen minimum zone of the open Arabian Sea: variability of oxygen and nitrite from daily to decadal timescales., Biogeosciences, 11, 2237–2261, 2014.

Barnier, B., Siefridt, L., and Marchesiello, P.: Thermal forcing for a global ocean circulation model using a three-year climatology of ECMWF analyses, Journal of Marine Systems, 6, 363–380, 1995.

Bianchi, D., Galbraith, E. D., Carozza, D. A., Mislan, K., and Stock, C. A.: Intensification of open-ocean oxygen depletion by vertically migrating animals, Nature Geoscience, 6, 545–548, 2013.

Bindoff, N. L., Cheung, W. W., Kairo, J. G., Arístegui, J., Guinder, V. A., Hallberg, R., Hilmi, N. J. M., Jiao, N., Karim, M. S., Levin, L., et al.: Changing ocean, marine ecosystems, and dependent communities, IPCC special report on the ocean and cryosphere in a changing climate, pp. 477–587, 2019.

Bograd, S. J., Buil, M. P., Di Lorenzo, E., Castro, C. G., Schroeder, I. D., Goericke, R., Anderson, C. R., Benitez-Nelson, C., and Whitney, F. A.: Changes in source waters to the Southern California Bight, Deep Sea Research Part II: Topical Studies in Oceanography, 112, 42–52, 2015.

Bopp, L., Resplandy, L., Orr, J. C., Doney, S. C., Dunne, J. P., Gehlen, M., Halloran, P., Heinze, C., Ilyina, T., Seferian, R., et al.: Multiple stressors of ocean ecosystems in the 21st century: projections with CMIP5 models, Biogeosciences, 10, 6225–6245, 2013.

Bopp, L., Resplandy, L., Untersee, A., Le Mezo, P., and Kageyama, M.: Ocean (de) oxygenation from the Last Glacial Maximum to the twenty-first century: insights from Earth System models, Philosophical Transactions of the Royal Society A: Mathematical, Physical and Engineering Sciences, 375, 20160 323, 2017.

Breitburg, D., Levin, L. A., Oschlies, A., Grégoire, M., Chavez, F. P., Conley, D. J., Garçon, V., Gilbert, D., Gutiérrez, D., Isensee, K., et al.: Declining oxygen in the global ocean and coastal waters, Science, 359, 2018.

Bristow, L. A., Callbeck, C. M., Larsen, M., Altabet, M. A., Dekaezemacker, J., Forth, M., Gauns, M., Glud, R. N., Kuypers, M. M., Lavik, G., et al.: N 2 production rates limited by nitrite availability in the Bay of Bengal oxygen minimum zone, Nature Geoscience, 10, 24–29, 2017.

Burt, J. A., Paparella, F., Al-Mansoori, N., Al-Mansoori, A., and Al-Jailani, H.: Causes and consequences of the 2017 coral bleaching event in the southern Persian/Arabian Gulf, Coral Reefs, 38, 567–589, 2019.

Carton, J. A. and Giese, B. S.: A reanalysis of ocean climate using Simple Ocean Data Assimilation (SODA), Monthly weather review, 136, 2999–3017, 2008.

Chaidez, V., Dreano, D., Agusti, S., Duarte, C. M., and Hoteit, I.: Decadal trends in Red Sea maximum surface temperature, Scientific Reports, 7, 1–8, 2017.

Cocco, V., Joos, F., Steinacher, M., Frölicher, T. L., Bopp, L., Dunne, J., Gehlen, M., Heinze, C., Orr, J., Oschlies, A., et al.: Oxygen and indicators of stress for marine life in multi-model global warming projections, Biogeosciences, 10, 1849–1868, 2013.

Codispoti, L., Brandes, J. A., Christensen, J., Devol, A., Naqvi, S., Paerl, H. W., and Yoshinari, T.: The oceanic fixed nitrogen and nitrous oxide budgets: Moving targets as we enter the anthropocene?, Scientia Marina, 65, 85–105, 2001.

Cummins, P. F. and Ross, T.: Secular trends in water properties at Station P in the northeast Pacific: an updated analysis, Progress in Oceanography, p. 102329, 2020.

Dai, A. and Trenberth, K. E.: Estimates of freshwater discharge from continents: Latitudinal and seasonal variations, Journal of hydrometeorology, 3, 660–687, 2002.

deCastro, M., Sousa, M., Santos, F., Dias, J., and Gómez-Gesteira, M.: How will Somali coastal upwelling evolve under future warming scenarios?, Scientific reports, 6, 1–9, 2016.

Deutsch, C., Brix, H., Ito, T., Frenzel, H., and Thompson, L.: Climate-forced variability of ocean hypoxia, science, 333, 336–339, 2011.

Deutsch, C., Berelson, W., Thunell, R., Weber, T., Tems, C., McManus, J., Crusius, J., Ito, T., Baumgartner, T., Ferreira, V., et al.: Centennial changes in North Pacific anoxia linked to tropical trade winds, Science, 345, 665–668, 2014.

Deutsch, C., Ferrel, A., Seibel, B., Pörtner, H.-O., and Huey, R. B.: Climate change tightens a metabolic constraint on marine habitats, Science, 348, 1132–1135, 2015.

do Rosário Gomes, H., Goes, J. I., Matondkar, S. P., Buskey, E. J., Basu, S., Parab, S., and Thoppil, P.: Massive outbreaks of Noctiluca scintillans blooms in the Arabian Sea due to spread of hypoxia, Nature Communications, 5, 1–8, 2014.

Frölicher, T. L., Rodgers, K. B., Stock, C. A., and Cheung, W. W.: Sources of uncertainties in 21st century projections of potential ocean ecosystem stressors, Global Biogeochemical Cycles, 30, 1224–1243, 2016.

Fu, W., Primeau, F., Keith Moore, J., Lindsay, K., and Randerson, J. T.: Reversal of increasing tropical ocean hypoxia trends with sustained climate warming, Global Biogeochemical Cycles, 32, 551–564, 2018.

Garcia, H. E. and Gordon, L. I.: Oxygen solubility in seawater: Better fitting equations, Limnology and oceanography, 37, 1307–1312, 1992.

Garcia, H. E., Boyer, T. P., Locarnini, R. A., Antonov, J. I., Mishonov, A. V., Baranova, O. K., Zweng, M. M., Reagan, J. R., Johnson, D. R., and Levitus, S.: World ocean atlas 2013. Volume 3, Dissolved oxygen, apparent oxygen utilization, and oxygen saturation, 2013a.

Garcia, H. E., Locarnini, R. A., Boyer, T. P., Antonov, J. I., Baranova, O. K., Zweng, M. M., Reagan, J. R., Johnson, D. R., Mishonov, A. V., and Levitus, S.: World ocean atlas 2013. Volume 4, Dissolved inorganic nutrients (phosphate, nitrate, silicate), 2013b.

Gobler, C. J. and Baumann, H.: Hypoxia and acidification in ocean ecosystems: coupled dynamics and effects on marine life, Biology letters, 12, 20150 976, 2016.

Goes, J. I., Thoppil, P. G., do R Gomes, H., and Fasullo, J. T.: Warming of the Eurasian landmass is making the Arabian Sea more productive, Science, 308, 545–547, 2005.

Goes, J. I., Tian, H., do Rosario Gomes, H., Anderson, O. R., Al-Hashmi, K., deRada, S., Luo, H., Al-Kharusi, L., Al-Azri, A., and Martinson, D. G.: Ecosystem state change in the Arabian Sea fuelled by the recent loss of snow over the Himalayan-Tibetan plateau region, Scientific reports, 10, 1–8, 2020.

Gopika, S., Izumo, T., Vialard, J., Lengaigne, M., Suresh, I., and Kumar, M. R.: Aliasing of the Indian Ocean externally-forced warming spatial pattern by internal climate variability, Climate Dynamics, 54, 1093–1111, 2020.

Griffies, S. M., Danabasoglu, G., Durack, P. J., Adcroft, A. J., Balaji, V., Boning, C. W., Chassignet, E. P., Curchitser, E., Deshayes, J., Drange, H., et al.: OMIP contribution to CMIP6: experimental and diagnostic protocol for the physical component of the Ocean Model Intercomparison Project, Geoscientific Model Development, pp. 3231–3296, 2016.

Gruber, N., Frenzel, H., Doney, S. C., Marchesiello, P., McWilliams, J. C., Moisan, J. R., Oram, J. J., Plattner, G.-K., and Stolzenbach, K. D.: Eddy-resolving simulation of plankton ecosystem dynamics in the California Current System, Deep Sea Research Part I: Oceanographic Research Papers, 53, 1483–1516, 2006.

Guieu, C., Al Azhar, M., Aumont, O., Mahowald, N., Lévy, M., Éthé, C., and Lachkar, Z.: Major impact of dust deposition on the productivity of the Arabian Sea, Geophysical Research Letters, 46, 6736–6744, 2019.

Hameau, A., Mignot, J., and Joos, F.: Assessment of time of emergence of anthropogenic deoxygenation and warming: insights from a CESM simulation from 850 to 2100 CE, Biogeosciences, 16, 1755–1780, 2019.

Huang, B., Liu, C., Banzon, V., Freeman, E., Graham, G., Hankins, B., Smith, T., and Zhang, H.-M.: Improvements of the daily optimum interpolation sea surface temperature (DOISST) version 2.1, Journal of Climate, 34, 2923–2939, 2021.

Ito, T., Minobe, S., Long, M. C., and Deutsch, C.: Upper ocean O2 trends: 1958–2015, Geophysical Research Letters, 44, 4214–4223, 2017.

Keller, D. P., Kriest, I., Koeve, W., and Oschlies, A.: Southern Ocean biological impacts on global ocean oxygen, Geophysical Research Letters, 43, 6469–6477, 2016.

Kendall, M. G.: Rank correlation methods., 1948.

Koné, V., Aumont, O., Lévy, M., and Resplandy, L.: Physical and biogeochemical controls of the phytoplankton seasonal cycle in the Indian Ocean: A modeling study, Indian Ocean Biogeochemical Processes and Ecological Variability, 185, 350, 2009.

Krishna, M., Prasad, M., Rao, D., Viswanadham, R., Sarma, V., and Reddy, N.: Export of dissolved inorganic nutrients to the northern Indian Ocean from the Indian monsoonal rivers during discharge period, Geochimica et Cosmochimica Acta, 172, 430–443, 2016.

Kumar, S. P., Roshin, R. P., Narvekar, J., Kumar, P. D., and Vivekanandan, E.: Response of the Arabian Sea to global warming and associated regional climate shift, Marine Environmental Research, 68, 217–222, 2009.

Kwiatkowski, L., Torres, O., Bopp, L., Aumont, O., Chamberlain, M., Christian, J. R., Dunne, J. P., Gehlen, M., Ilyina, T., John, J. G., et al.: Twenty-first century ocean warming, acidification, deoxygenation, and upper-ocean nutrient and primary production decline from CMIP6 model projections, Biogeosciences, 17, 3439–3470, 2020.

Lachkar, Z., Smith, S., Lévy, M., and Pauluis, O.: Eddies reduce denitrification and compress habitats in the Arabian Sea, Geophysical Research Letters, 43, 9148–9156, 2016.

Lachkar, Z., Lévy, M., and Smith, S.: Intensification and deepening of the Arabian Sea oxygen minimum zone in response to increase in Indian monsoon wind intensity., Biogeosciences, 15, 2018.

Lachkar, Z., Lévy, M., and Smith, K.: Strong intensification of the Arabian Sea oxygen minimum zone in response to Arabian Gulf warming, Geophysical Research Letters, 46, 5420–5429, 2019.

Laffoley, D. D. and Baxter, J.: Ocean Deoxygenation: Everyone's Problem-Causes, Impacts, Consequences and Solutions, IUCN, 2019.

Large, W. G. and Yeager, S. G.: Diurnal to decadal global forcing for ocean and sea-ice models: The data sets and flux climatologies, 2004.

Large, W. G., McWilliams, J. C., and Doney, S. C.: Oceanic vertical mixing: A review and a model with a nonlocal boundary layer parameterization, Reviews of Geophysics, 32, 363–403, 1994.

Levin, L. A.: Manifestation, drivers, and emergence of open ocean deoxygenation, Annual review of marine science, 10, 229–260, 2018.

Long, M. C., Deutsch, C., and Ito, T.: Finding forced trends in oceanic oxygen, Global Biogeochemical Cycles, 30, 381–397, 2016.

Lumpkin, R. and Johnson, G. C.: Global ocean surface velocities from drifters: Mean, variance, El Niño–Southern Oscillation response, and seasonal cycle, Journal of Geophysical Research: Oceans, 118, 2992–3006, 2013.

Mann, H. B.: Nonparametric tests against trend, Econometrica: Journal of the econometric society, pp. 245–259, 1945.

Marchesiello, P., Debreu, L., and Couvelard, X.: Spurious diapycnal mixing in terrain-following coordinate models: The problem and a solution, Ocean Modelling, 26, 156–169, 2009.

McCreary, J. P., Yu, Z., Hood, R. R., Vinaychandran, P., Furue, R., Ishida, A., and Richards, K. J.: Dynamics of the Indian-Ocean oxygen minimum zones, Progress in Oceanography, 112, 15–37, 2013.

Merchant, C. J., Embury, O., Roberts-Jones, J., Fiedler, E., Bulgin, C. E., Corlett, G. K., Good, S., McLaren, A., Rayner, N., Morak-Bozzo, S., et al.: Sea surface temperature datasets for climate applications from Phase 1 of the European Space Agency Climate Change Initiative (SST CCI), Geoscience Data Journal, 1, 179–191, 2014.

Miller, S. H., Breitburg, D. L., Burrell, R. B., and Keppel, A. G.: Acidification increases sensitivity to hypoxia in important forage fishes, Marine Ecology Progress Series, 549, 1–8, 2016.

Oschlies, A., Brandt, P., Stramma, L., and Schmidtko, S.: Drivers and mechanisms of ocean deoxygenation, Nature Geoscience, 11, 467–473, 2018.

Piontkovski, S. and Al-Oufi, H.: The Omani shelf hypoxia and the warming Arabian Sea, International Journal of Environmental Studies, 72, 256–264, 2015.

Praveen, V., Ajayamohan, R., Valsala, V., and Sandeep, S.: Intensification of upwelling along Oman coast in a warming scenario, Geophysical Research Letters, 43, 7581–7589, 2016.

Queste, B. Y., Vic, C., Heywood, K. J., and Piontkovski, S. A.: Physical controls on oxygen distribution and denitrification potential in the north west Arabian Sea, Geophysical Research Letters, 45, 4143–4152, 2018.

Rabalais, N. N., Turner, R. E., and Wiseman Jr, W. J.: Gulf of Mexico hypoxia, aka "The dead zone", Annual Review of ecology and Systematics, 33, 235–263, 2002.

Ramesh, R., Purvaja, G., and Subramanian, V.: Carbon and phosphorus transport by the major Indian rivers, Journal of Biogeography, pp. 409–415, 1995.

Rayner, N., Parker, D. E., Horton, E., Folland, C. K., Alexander, L. V., Rowell, D., Kent, E. C., and Kaplan, A.: Global analyses of sea surface temperature, sea ice, and night marine air temperature since the late nineteenth century, Journal of Geophysical Research: Atmospheres, 108, 2003.

Resplandy, L., Lévy, M., Bopp, L., Echevin, V., Pous, S., Sarma, V., and Kumar, D.: Controlling factors of the oxygen balance in the Arabian Sea's OMZ, Biogeosciences, 9, 5095–5109, 2012.

Robinson, C.: Microbial respiration, the engine of ocean deoxygenation, Frontiers in Marine Science, 5, 533, 2019.

Roxy, M. K., Modi, A., Murtugudde, R., Valsala, V., Panickal, S., Prasanna Kumar, S., Ravichandran, M., Vichi, M., and Lévy, M.: A reduction in marine primary productivity driven by rapid warming over the tropical Indian Ocean, Geophysical Research Letters, 43, 826–833, 2016.

Sandeep, S. and Ajayamohan, R.: Poleward shift in Indian summer monsoon low level jetstream under global warming, Climate Dynamics, 45, 337–351, 2015.

Schmidtko, S., Stramma, L., and Visbeck, M.: Decline in global oceanic oxygen content during the past five decades, Nature, 542, 335–339, 2017.

Schott, F. A., Xie, S.-P., and McCreary Jr, J. P.: Indian Ocean circulation and climate variability, Reviews of Geophysics, 47, 2009.

Séférian, R., Berthet, S., Yool, A., Palmiéri, J., Bopp, L., Tagliabue, A., Kwiatkowski, L., Aumont, O., et al.: Tracking improvement in simulated marine biogeochemistry between CMIP5 and CMIP6, Current Climate Change Reports, 10, 2020.

Shchepetkin, A. F. and McWilliams, J. C.: The regional oceanic modeling system (ROMS): a split-explicit, free-surface, topography-following-coordinate oceanic model, Ocean modelling, 9, 347–404, 2005.

Sooraj, K., Terray, P., and Mujumdar, M.: Global warming and the weakening of the Asian summer monsoon circulation: assessments from the CMIP5 models, Climate Dynamics, 45, 233–252, 2015.

Stewart, K., Kim, W., Urakawa, S., Hogg, A. M., Yeager, S., Tsujino, H., Nakano, H., Kiss, A., and Danabasoglu, G.: JRA55-do-based repeat year forcing datasets for driving ocean–sea-ice models, Ocean Modelling, 147, 101 557, 2020.

Stramma, L., Johnson, G. C., Sprintall, J., and Mohrholz, V.: Expanding oxygen-minimum zones in the tropical oceans, science, 320, 655–658, 2008.

Strong, A. E., Liu, G., Skirving, W., and Eakin, C. M.: NOAA's Coral Reef Watch program from satellite observations, Annals of GIS, 17, 83–92, 2011.

Swapna, P., Jyoti, J., Krishnan, R., Sandeep, N., and Griffies, S.: Multidecadal weakening of Indian summer monsoon circulation induces an increasing northern Indian Ocean sea level, Geophysical Research Letters, 44, 10–560, 2017.

Taylor, K. E.: Summarizing multiple aspects of model performance in a single diagram, Journal of Geophysical Research: Atmospheres, 106, 7183–7192, 2001.

Vallivattathillam, P., Iyyappan, S., Lengaigne, M., Ethé, C., Vialard, J., Levy, M., Suresh, N., Aumont, O., Resplandy, L., Naik, H., et al.: Positive Indian Ocean Dipole events prevent anoxia off the west coast of India, Biogeosciences, 14, 1541–1559, 2017.

Vaquer-Sunyer, R. and Duarte, C. M.: Thresholds of hypoxia for marine biodiversity, Proceedings of the National Academy of Sciences, 105, 15 452–15 457, 2008.

Wang, B., Liu, J., Kim, H.-J., Webster, P. J., Yim, S.-Y., and Xiang, B.: Northern Hemisphere summer monsoon intensified by mega-El Niño/southern oscillation and Atlantic multidecadal oscillation, Proceedings of the National Academy of Sciences, 110, 5347–5352, 2013.

Whitney, F. A., Freeland, H. J., and Robert, M.: Persistently declining oxygen levels in the interior waters of the eastern subarctic Pacific, Progress in Oceanography, 75, 179–199, 2007.